

RESEARCH PAPER



# Design and synthesis of novel quinazolinones conjugated ibuprofen, indole acetamide, or thioacetohydrazide as selective COX-2 inhibitors: anti-inflammatory, analgesic and anticancer activities

Asmaa Sakr<sup>a</sup>, Samar Rezaq<sup>b,c,d,e,f</sup>, Samy M. Ibrahim<sup>a</sup>, Eman Soliman<sup>b</sup>, Mohamed M. Baraka<sup>a</sup>, Damian G. Romero<sup>c,d,e,f</sup> and Hend Kothayer<sup>a</sup>

<sup>a</sup>Department of Medicinal Chemistry, Faculty of Pharmacy, Zagazig University, Zagazig, Egypt; <sup>b</sup>Department of Pharmacology and Toxicology, Faculty of Pharmacy, Zagazig University, Zagazig, Egypt; <sup>c</sup>Department of Cell and Molecular Biology, University of Mississippi Medical Center, Jackson, MS, USA; <sup>d</sup>Mississippi Center of Excellence in Perinatal Research, University of Mississippi Medical Center, Jackson, MS, USA; <sup>e</sup>Women's Health Research Center, University of Mississippi Medical Center, Jackson, MS, USA; <sup>f</sup>Cardiovascular-Renal Research Center, University of Mississippi Medical Center, Jackson, MS, USA

## ABSTRACT

Novel quinazolinones conjugated with indole acetamide (**4a–c**), ibuprofen (**7a–e**), or thioacetohydrazide (**13a,b**, and **14a–d**) were designed to increase COX-2 selectivity. The three synthesised series exhibited superior COX-2 selectivity compared with the previously reported quinazolinones and their NSAID analogue and had equipotent COX-2 selectivity as celecoxib. Compared with celecoxib, **4b**, **7c**, and **13b** showed similar anti-inflammatory activity *in vivo*, while **13b** and **14a** showed superior inhibition of the inflammatory mediator nitric oxide, and **7** showed greater antioxidant potential in macrophages cells. Moreover, all selected compounds showed improved analgesic activity and **13b** completely abolished the pain response. Additionally, compound **4a** showed anticancer activity in tested cell lines HCT116, HT29, and HCA7. Docking results were consistent with COX-1/2 enzyme assay results. *In silico* studies suggest their high oral bioavailability. The overall findings for compounds (**4a,b**, **7c**, **13b**, and **14c**) support their potential role as anti-inflammatory agents.

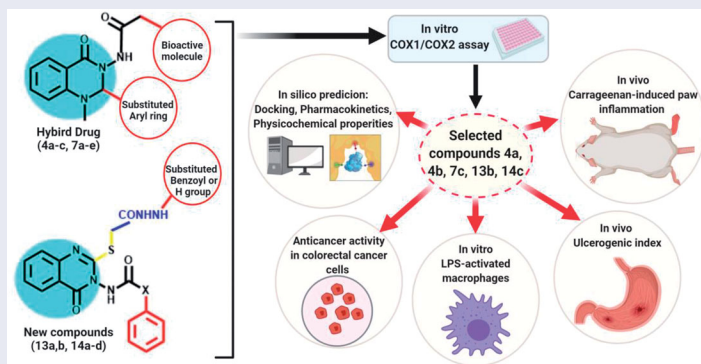
## ARTICLE HISTORY

Received 19 January 2021  
Revised 29 June 2021  
Accepted 13 July 2021

## KEYWORDS

COX-2 inhibition; quinazolinone; anti-inflammatory; molecular modelling; Anticancer

## GRAPHICAL ABSTRACT




## 1. Introduction

Inflammation is a defensive mechanism as a response by the body to combat infections, chemicals or physical tissue injury<sup>1</sup>. The pathophysiology of pain is characterised by the release inflammatory mediators to initiate pain sensation, oedema, and other hallmarks of inflammation. Steroids are efficient in reducing inflammation and its associated pain however their use is complicated both by the wide range of adverse effects and by the necessity of their gradual withdrawal following the end of the

treatment course<sup>2</sup>. While nonsteroidal anti-inflammatory drugs, (NSAIDs) such as indomethacin, ibuprofen, and diclofenac, have a relatively safe response profile, their long-term consumption is associated with severe gastrointestinal and renal side effects<sup>3,4</sup>.

Recent studies associated with the discovery of cyclooxygenase isozymes (COX-1/2) have helped advance the current understanding of inflammatory mechanisms<sup>5</sup>. The inhibition of COX-1 is the main cause of detrimental NSAID-associated gastrointestinal and renal side effects, thus “coxibs” were synthesised as selective

**CONTACT** Hend Kothayer  [hendo1311@hotmail.com](mailto:hendo1311@hotmail.com), HKElhamalawy@pharmacy.zu.edu.eg  Department of Medicinal Chemistry, Faculty of Pharmacy, Zagazig University, 44519, Zagazig, Egypt

 Supplemental data for this article can be accessed [here](#).

© 2021 The Author(s). Published by Informa UK Limited, trading as Taylor & Francis Group.

This is an Open Access article distributed under the terms of the Creative Commons Attribution License (<http://creativecommons.org/licenses/by/4.0/>), which permits unrestricted use, distribution, and reproduction in any medium, provided the original work is properly cited.

inhibitors for COX-2, which are themselves associated with cardiovascular toxicity<sup>6,7</sup>. Recently, however, these adverse effects are expected to be drug-dependent rather than class-dependent<sup>8</sup>. Moreover, the COX-2 isozyme is overexpressed in human colon, gastric, hepatocellular, breast, ovarian, lung, and prostate cancers, and its inhibition is associated with a lower risk of cancer development<sup>9,10</sup>. In this way, COX-2 can be considered to be a potential anticancer target, specifically in cancer cells in which it is overexpressed. Consequently, there is a continuous need for the development of new selective COX-2 inhibitors with an improved gastric, and renal profiles, and fewer consequential side effects.

Recently, several compounds have been synthesised and evaluated as selective COX-2 inhibitors. Their common structural features involve the presence of two adjoining aryl rings attached to

a central heterocyclic moiety (V-shape) with the possibility of introduction of a linker, either an ester<sup>11</sup> or an amide<sup>12,13</sup>, between one of the aryl rings and the central heterocycle.

In continuation of our previous study, herein, we made further modifications to our previous successfully designed anti-inflammatory quinazolinones (I) (Figure 1), in order to increase their selectivity towards COX-2 inhibition<sup>13</sup>. In our current design, we kept the following: (a) the 2,3 diaryl-heterocyclic moiety (V-shape) to maintain the common structural integrity of selective COX-2 inhibitors<sup>10,11,13</sup>, (b) quinazolinone as the central heterocyclic ring due to its remarkable anti-inflammatory and analgesic activities<sup>13,14</sup>, and (c) the aryl ring at position 3 connected via an amide linker which may potentiate target interactions. Additionally, the introduction of the amide linker to the compounds allows for a bulkier

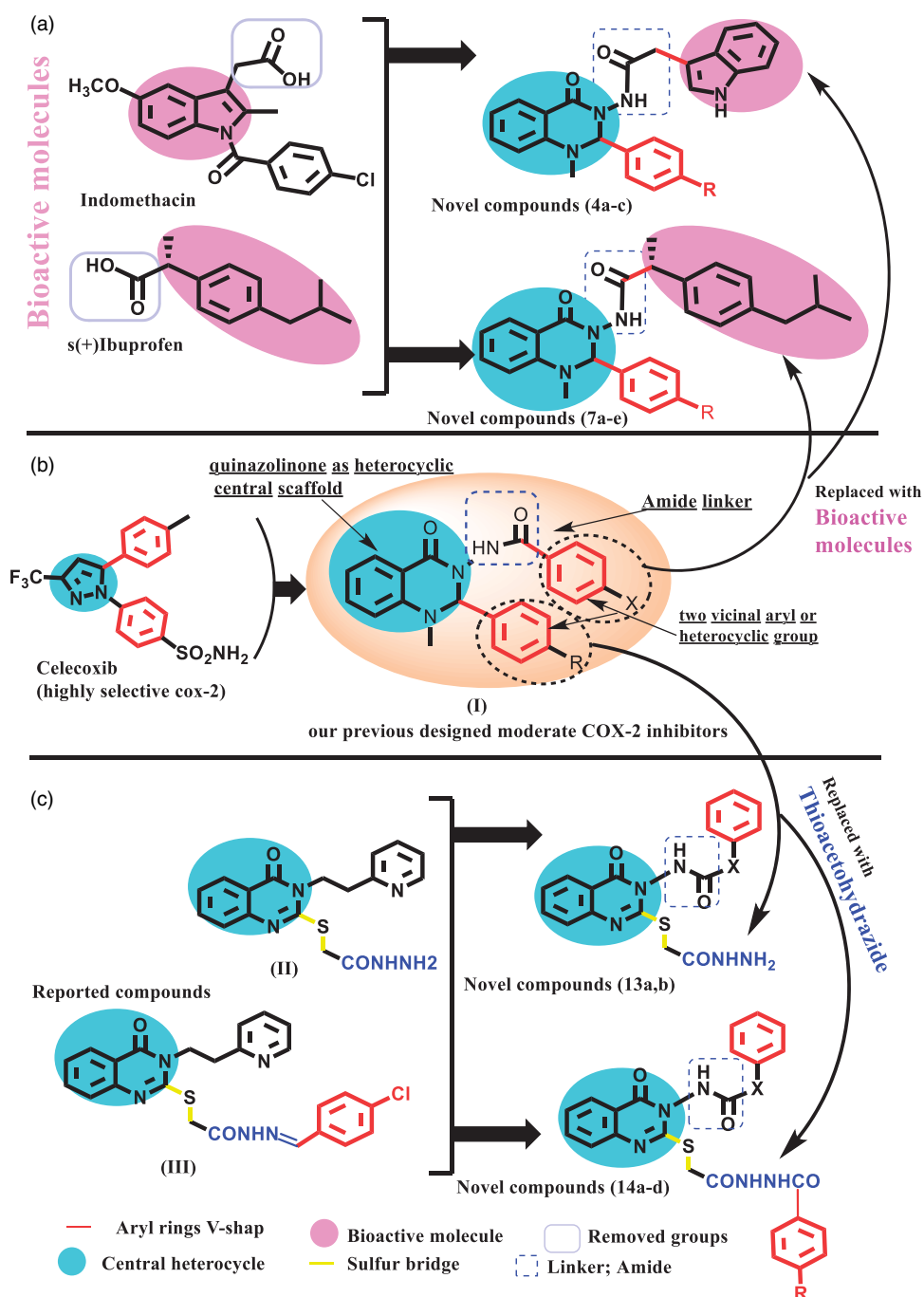


**Figure 1.** (a) Molecular design for hybrid bioactive novel compounds; (b) our previous designed moderate COX-2 from general structure selective COX-2; (c) Molecular design incorporates thioacetohydrazide novel compounds.

structure, and thus, more favourable for COX-2 active site entry, which is approximately 20% larger than the COX-1 active site<sup>12,13</sup>.

The approach of Schemes 1 and 2 is to explore the effect of incorporating a bioactive anti-inflammatory moiety (either indole acetamide (as indomethacin-alternative) or ibuprofen, respectively) (Figure 1), as the aryl ring attached to position 3 of the quinazolinone scaffold. The latter modification not only could increase COX-2 selectivity due to stoichiometric changes but also could help to explore further possible target interactions.

Both the classic non-selective COX inhibitors indomethacin and ibuprofen bind tightly to the COX active site. However, we faced some difficulty in synthesising the required indomethacin hydrazide, so our design was amended by incorporating indole-3-acetic acid instead of indomethacin. Aside from indomethacin, indole derivatives also possess significant anti-inflammatory activity<sup>15–18</sup>. Moreover, the benzoyl oxygen of indomethacin has been considered to be responsible for increased COX-1 affinity as its 4-bromobenzyl analogue exhibited high COX-2 selectivity, albeit without a benzoyl oxygen<sup>19</sup>. Therefore, in our design, we chose indole acetamide as an indomethacin alternative to overcome this problem. Additionally, to minimise the possible detrimental gastric effects, we masked the carboxylic acid group of both the indomethacin-alternative moiety and ibuprofen, which is responsible for salt bridge formation with Arg120 residue of the COX-1 active site causing their gastric mucosal side effects<sup>13,19</sup>.

In Scheme 3, the pivotal feature of our approach was to study the shifting effect of phenyl ring located at position 2 of the quinazolinone moiety, via incorporation of a thioacetohydrazide linker, on both COX-2 selectivity and potency. Recent studies have shown advantages in the addition of a sulphur bridge at position 2 of the quinazolinone moiety in improving its anti-inflammatory activity<sup>20</sup> (**II**, **III**) (Figure 1). Additionally, compounds containing an amide group showed superior *in-vivo* activity because they can easily cross the biological membrane<sup>21</sup>. Moreover, the hydrazide moiety at this position is able to make extra binding interactions with nearby amino acids within the COX active site.

Another focus of our investigation was to add flexibility between the quinazolinone scaffold and the aryl moiety at position 3 by the introduction of a rotatable bond next to the amide. This conformational freedom from the added flexibility may influence the potency and the selectivity of the newly synthesised compounds.

The newly synthesised compounds (**4a–c**, **7a–e**, **13a,b**, and **14a–d**) were evaluated for their COX-1/COX-2 selectivity using *in vitro* and *in vivo* assays to test their anti-inflammatory and antioxidant potential, and to investigate their ulcerogenic activity (UI) profile. To evaluate their possible anticancer activity through COX-2, we utilised cancer cell lines that have low, medium, or high COX-2 expression levels. Docking and *in silico* studies were used to predict their binding modes with COX-1/COX2, physicochemical properties, and pharmacokinetic profiles.

## 2. Materials and methods

### 2.1. Chemistry

Melting points (°C) were detected on a Gallenkamp melting point apparatus (London, UK), and are uncorrected. Elemental analyses, and mass spectra were performed in the Microanalytical Centre, Faculty of Science, Cairo University, Giza, Egypt. NMR spectra were performed in NMR Unit, Faculty of Pharmacy, Mansoura University, Egypt, or Microanalytical Centre, Faculty of Pharmacy, Cairo

University, Egypt or Microanalytical Centre, Faculty of Science, Zagazig University, Egypt. NMR Spectra were recorded on Bruker high-performance Digital FT-NMR spectrometer avance III 400 MHz using dimethyl sulphoxide (DMSO)-d<sub>6</sub> or pyridine (Pyr)-d<sub>6</sub> as solvent and tetramethylsilane (TMS) as an internal standard (chemical shift in  $\delta$ , ppm). Mass spectra were determined using a GC/MS Shimadzu Qp-2010 plus (Shimadzu Corporation, Tokyo, Japan). Elemental analyses were established using the Vario EL-III (Elementar) CHNS analyser (Hanau, Germany). All reactions were continuously monitored by thin-layer chromatography (TLC) using silica gel 60 GF245 (E-Merck, Germany) and were detected by UV-lamp at wavelength ( $\lambda$ ) 254 nm. Reagents and solvents were purchased from commercial suppliers and used as received. The isatoic anhydride was purchased from Sigma Aldrich (MO, USA) and ibuprofen was gifted from El-Qahera for pharmaceutical and chemical industries (Cairo, Egypt). The compound (**1**) was prepared as reported before<sup>22</sup>. The hydrazides (**2**, **5**, **9a**, and **9b**) were synthesised starting from their corresponding acids using previously reported procedures<sup>23–26</sup>. Compounds (**10a**, **b–11a**, **b**) were synthesised according to procedures previously described in the literatures<sup>27,28</sup>.

#### 2.1.1. N'-(2-(1H-indol-3-yl)acetyl)-2-(methylamino) benzohydrazide (**3**)

A mixture of indole-3-acetic acid hydrazide (**2**, 6 g, 0.031 mole), and N-methyl isatoic anhydride (**1**, 0.031 mole) in absolute ethanol (50 ml) acidified with glacial acetic acid (2 ml) was refluxed for 12 h; the formed precipitate upon reflux was filtered while hot to provide compound (**3**) as fluffy white powder.

Yield 70%, m.p. 187–191 °C, <sup>1</sup>H NMR (DMSO-d<sub>6</sub>)  $\delta$ : 2.78 (3H, d,  $J$  = 4.92, NCH<sub>3</sub>), 3.63 (2H, s, CH<sub>2</sub>CO), 6.56 (1H, t,  $J$  = 7.44, benzo hydrazide-C<sub>5</sub>-H), 6.66 (1H, d,  $J$  = 8.32, benzo hydrazide-C<sub>3</sub>-H), 7.00 (1H, t,  $J$  = 7.4, indole-C<sub>5</sub>-H), 7.09 (1H, t,  $J$  = 7.16, indole-C<sub>6</sub>-H), 7.28–7.36 (3H, m, indole-C<sub>2</sub>-H, benzo hydrazide-C<sub>7</sub>-H, indole-C<sub>7</sub>-H), 7.48 (1H, bs, NHCH<sub>3</sub>, exch.), 7.58 (1H, d,  $J$  = 7.64, indole-C<sub>4</sub>-H), 7.64 (1H, d,  $J$  = 7.8, benzo hydrazide-C<sub>6</sub>-H), 9.97 (1H, s, CONH, exch.), 10.06 (1H, s, CONH, exch.), 10.89 (1H, s, indole NH, exch.).

#### 2.1.2. General method for synthesis of N-(2-(4-substitutedphenyl)-1-methyl-4-oxo-1,4-dihydroquinazolin-3(2H)-yl)-2-(1H-indol-3-yl)acetamide (**4a–c**)

A mixture of N'-(2-(1H-indol-3-yl)acetyl)-2-(methylamino) benzohydrazide (methylamino) benzohydrazide (**3**, 4 g, 0.025 mole), and appropriate aromatic aldehyde in absolute ethanol acidified with glacial acetic acid (2 ml) was refluxed for 8–24 h. The reaction mixture concentrated to its half volume then:

For the chloride derivative (**4a**); after 8 h, the reaction mixture cooled, H<sub>2</sub>O drops were added then left in refrigerator for 6 h. The formed crystals were filtered and recrystallized from ethanol/H<sub>2</sub>O (5:2) under 20 °C, to obtain compound **4a**.

Or, for nitro derivatives (**4b**); after 12 h, the yellow ppt. formed after concentration reaction mixture on hot was filtered, dried and washed several times with petroleum ether to yield pure compound **4b**.

Or, for methoxy derivative (**4c**); after 24 h, the reaction mixture was cooled, H<sub>2</sub>O drops were added then left in refrigerator for 6 h. The formed semisolid was scratching with glass rod several times with diethyl ether, kept in closed container with diethyl ether and returned to refrigerator under 4 °C for 48 h, to yield **4c**.

### 2.1.3. *N*-(2-(4-chlorophenyl)-1-methyl-4-oxo-1,4-dihydroquinazolin-3(2H)-yl)-2-(1H-indol-3-yl)acetamide (4a)

White crystals, yield 36%, m.p. 211–214 °C. <sup>1</sup>H NMR (DMSO-d<sub>6</sub>) δ: 2.77 (3H, s, NCH<sub>3</sub>), 3.58 (2H, q, J = 4.92, CH<sub>2</sub>CO), 5.78 (1H, s, NCHN), 6.70 (1H, d, J = 8.32, quinazolinone-C<sub>8</sub>-H), 6.86 (1H, t, J = 7.48, quinazolinone-C<sub>6</sub>-H), 6.98 (1H, t, J = 7.6, indole-C<sub>5</sub>-H), 7.09 (1H, t, J = 7.36, indole -C<sub>6</sub>-H), 7.23 (3H, d, J = 8.44, indole-C<sub>2</sub>-H, phenyl-C<sub>2,6</sub>-H), 7.35–7.47 (4H, m, indole-C<sub>7</sub>-H, phenyl-C<sub>3,5</sub>-H, quinazolinone-C<sub>7</sub>-H), 7.52 (1H, d, J = 7.84, indole-C<sub>4</sub>-H), 7.80 (1H, d, J = 6.48, quinazolinone-C<sub>5</sub>-H), 10.43 (1H, s, CONH, exch.), 10.90 (1H, s, indole NH, exch.). <sup>13</sup>C NMR (DMSO-d<sub>6</sub>) δ: 30.80 (CH<sub>2</sub>), 35.47 (NCH<sub>3</sub>), 79.37 (NCHN), 108.28 (ArCH), 111.76 (ArCH), 112.90 (ArCH), 115.03 (ArCH), 118.46 (ArCH), 118.83 (ArCH), 119.17 (ArCH), 121.50 (ArCH), 124.41 (ArCH), 127.59 (ArCH), 128.50 (ArCH), 128.99 (ArC), 129.05 (ArC), 134.19 (ArC), 135.13 (ArC), 136.45 (ArC), 136.51 (ArC), 147.03 (ArC), 160.85 (ArC), 170.13 (ArC). MS, m/z: 445 (M<sup>+</sup>), 447 (M<sup>+</sup>+2). Analysis calcd. for C<sub>25</sub>H<sub>21</sub>ClN<sub>4</sub>O<sub>2</sub>: C, 67.49; H, 4.76; N, 12.59. Found: C, 67.46; H, 4.80; N, 12.33.

### 2.1.4. 2-(1 h-indol-3-yl)-N-(1-methyl-2-(4-nitrophenyl)-4-oxo-1,4-dihydroquinazolin-3(2H)-yl)acetamide (4b)

Yellow powder, yield 71%, m.p. 239–243 °C. <sup>1</sup>H NMR (DMSO-d<sub>6</sub>) δ: 2.8 (3H, s, NCH<sub>3</sub>), 3.57 (2H, s, CH<sub>2</sub>CO), 5.96 (1H, s, NCHN), 6.73 (1H, d, J = 8.28, quinazolinone-C<sub>8</sub>-H), 6.89 (1H, t, J = 7.44, quinazolinone-C<sub>6</sub>-H), 6.96 (1H, t, J = 7.56, indole-C<sub>5</sub>-H), 7.08 (1H, t, J = 7.2, indole-C<sub>6</sub>-H), 7.22 (1H, bs, indole-C<sub>2</sub>-H), 7.35 (1H, d, J = 8.08, indole-C<sub>7</sub>-H), 7.46–7.50 (4H, m, indole-C<sub>4</sub>-H, quinazolinone-C<sub>7</sub>-H, phenyl-C<sub>2,6</sub>-H), 7.81 (1H, d, J = 7.64, quinazolinone-C<sub>5</sub>-H), 8.15 (2H, d, J = 8.68, phenyl-C<sub>3,5</sub>-H), 10.48 (1H, s, CONH, exch.), 10.89 (1H, s, Indole NH, exch.). <sup>13</sup>C NMR (DMSO-d<sub>6</sub>) δ: 30.85 (SCH<sub>2</sub>), 35.61 (NCH<sub>3</sub>), 79.06 (NCHN), 108.20 (ArCH), 111.75 (ArCH), 113.16 (ArCH), 115.14 (ArCH), 118.78 (ArCH), 119.13 (ArCH), 121.47 (ArCH), 124.18 (ArCH), 124.40 (ArCH), 127.58 (ArCH), 128.56 (ArCH), 128.61 (ArC), 129.05 (ArC), 135.20 (ArC), 136.51 (ArC), 144.59 (ArC), 146.91 (ArC), 148.34 (ArC), 160.74 (ArC), 170.15 (ArC). MS, m/z: 455 (M<sup>+</sup>). Analysis calcd. for C<sub>25</sub>H<sub>21</sub>N<sub>5</sub>O<sub>4</sub>: C, 65.93; H, 4.65; N, 15.38. Found: C, 65.91; H, 4.85; N, 15.23.

### 2.1.5. 2-(1 h-indol-3-yl)-N-(2-(4-methoxyphenyl)-1-methyl-4-oxo-1,4-dihydroquinazolin-3(2H)-yl)acetamide (4c)

Yellow powder, yield 36%, m.p. 83–85 °C. <sup>1</sup>H NMR (DMSO-d<sub>6</sub>) δ: 2.74 (3H, s, NCH<sub>3</sub>), 3.58 (2H, d, J = 7.28, COCH<sub>2</sub>), 3.74 (3H, s, OCH<sub>3</sub>), 5.68 (1H, s, NCHN), 6.68 (1H, d, J = 8.28, quinazolinone-C<sub>8</sub>-H), 6.83–6.89 (3H, m, quinazolinone-C<sub>6</sub>-H, phenyl-C<sub>3,5</sub>-H), 6.99 (1H, t, J = 7.36, indole-C<sub>5</sub>-H), 7.08–7.14 (3H, m, indole-C<sub>6</sub>-H, phenyl-C<sub>2,6</sub>-H), 7.23 (1H, bs, indole-C<sub>2</sub>-H), 7.37 (1H, d, J = 8.32, indole-C<sub>7</sub>-H), 7.43 (1H, t, J = 7, quinazolinone-C<sub>7</sub>-H), 7.54 (1H, d, J = 7.84, indole-C<sub>4</sub>-H), 7.80 (1H, d, J = 6.36, quinazolinone-C<sub>5</sub>-H), 10.39 (1H, s, CONH, exch.), 10.89 (1H, s, Indole NH, exch.). <sup>13</sup>C NMR (DMSO-d<sub>6</sub>) δ: 30.76 (CH<sub>2</sub>), 35.38 (NCH<sub>3</sub>), 55.58 (OCH<sub>3</sub>), 79.74 (NCHN), 108.39 (ArCH), 111.75 (ArCH), 112.71 (ArCH), 114.34 (ArCH), 115.07 (ArCH), 118.15 (ArCH), 118.82 (ArCH), 119.21 (ArCH), 121.49 (ArCH), 124.39 (ArCH), 127.61 (ArCH), 128.44 (ArC), 128.79 (ArC), 129.53 (ArC), 135.00 (ArC), 136.51 (ArC), 147.24 (ArC), 160.23 (ArC), 161.00 (ArC), 170.07 (ArC). MS, m/z: 441 (M<sup>+</sup>). Analysis calcd. for C<sub>26</sub>H<sub>24</sub>N<sub>4</sub>O<sub>3</sub>: C, 70.89; H, 5.49; N, 12.72. Found: C, 70.58; H, 5.66; N, 12.50.

### 2.1.6. *N'*-(2-(4-isobutylphenyl)propanoyl)-2-(methylamino) benzo-hydrazide (6)

A mixture of *N*-methyl isatoic anhydride (**1**, 20 gm, 0.0112 mole) and R/S ibuprofen hydrazide (**5**, 0.0112 mole) in absolute ethanol (250 ml) acidified by glacial acetic acid (4 ml) was refluxed for 3 h. The reaction mixture was cooled, and a white solid was precipitated immediately, filtered with suction system and dried to give the target compound **6**.

White powder, yield 85%, m.p. 148–150 °C. <sup>1</sup>H NMR (DMSO-d<sub>6</sub>) δ: 0.87 (6H, d, J = 6.6, CH<sub>3</sub>CHCH<sub>3</sub>), 1.39 (3H, d, J = 7, CH<sub>3</sub>CHCO), 1.79–1.84 (1H, m, CH<sub>3</sub>CHCH<sub>3</sub>), 2.42 (2H, d, J = 7.12, CHCH<sub>2</sub>), 2.78 (3H, d, J = 4.88, NCH<sub>3</sub>), 3.71 (1H, q, J = 7.04, CH<sub>3</sub>CHCO), 6.55 (1H, t, J = 7.4, benzo hydrazide-C<sub>5</sub>-H), 6.65 (1H, d, J = 8.32, benzo hydrazide-C<sub>3</sub>-H), 7.08 (2H, d, J = 7.64, ibuprofen phenyl-C<sub>2,6</sub>-H), 7.29–7.34 (3H, m, benzo hydrazide-C<sub>4</sub>-H, ibuprofen phenyl-C<sub>3,5</sub>-H), 7.45 (1H, bs, NHCH<sub>3</sub>, exch.), 7.58 (1H, d, J = 7.48, benzo hydrazide-C<sub>6</sub>-H), 9.97 (1H, s, CONH, exch.), 10.05 (1H, s, CONH, exch.).

### 2.1.7. General method for synthesis of *N*-(2-(4-substitutedphenyl)-1-methyl-4-oxo-1,4-dihydroquinazolin-3(2H)-yl)-2-(4-isobutylphenyl) propenamide (7a-e)

A mixture of *N'*-(2-(4-isobutylphenyl) propanoyl)-2-(methylamino) benzohydrazide (**6**, 8 g, 0.023 mole), and appropriate aromatic aldehyde (0.023 mole) in glacial acetic acid (10 ml), was refluxed at 120 °C for 8 h. The reaction mixture was concentrated to its half, cooled, drops of H<sub>2</sub>O were added, put in refrigerator for 6 h then:

For the chloride derivative compound (**7b**); the white semi solid precipitated obtained was dried after removal of all supernatant, then dissolved in ethanol/H<sub>2</sub>O (5:2) and kept in refrigerator under 20 °C for 6 h. The resulted crystals were filtered and dried to give the desired compound **7b**.

For the other derivatives compounds (**7a**, **7c-e**), the yellow to brown semisolid precipitates formed after drying and removal of supernatant were dissolved in methanol (least amount) to form a concentrated solution and keep scratching with glass rod to give pure solid precipitated.

### 2.1.8. 2-(4-Isobutylphenyl)-N-(1-methyl-4-oxo-2-phenyl-1,4-dihydroquinazolin-3(2H)-yl) propenamide (7a)

White powder, yield 40%, m.p. 85–89 °C. <sup>1</sup>H NMR (DMSO-d<sub>6</sub>) δ: 0.86–0.89 (6H, m, CH<sub>3</sub>CHCH<sub>3</sub>), 1.31–1.35 (3H, m, CH<sub>3</sub>CHCO), 1.81–1.86 (1H, m, CH<sub>3</sub>CHCH<sub>3</sub>), 2.43 (2H, t, J = 2.72, CHCH<sub>2</sub>), 2.71, 2.78 (3H, s, NCH<sub>3</sub>), 3.63–3.69 (1H, m, CH<sub>3</sub>CHCO), 5.57, 5.81 (1H, d, s, NCHN), 6.72 (1H, d, J = 8.28, quinazolinone-C<sub>8</sub>-H), 6.85 (1H, q, J = 4, quinazolinone -C<sub>6</sub>-H), 6.99 (1H, d, J = 7.4, phenyl-C<sub>2</sub>-H), 7.09 (2H, t, J = 8.6, ibuprofen phenyl-C<sub>3,5</sub>-H), 7.21–7.27 (4H, m, ibuprofen phenyl-C<sub>2,6</sub>-H, phenyl-C<sub>4</sub>-H, phenyl-C<sub>6</sub>-H), 7.29–7.35 (2H, m, phenyl-C<sub>3,5</sub>-H), 7.45 (1H, q, J = 5.2, quinazolinone-C<sub>7</sub>-H), 7.77 (1H, q, J = 7.56, quinazolinone-C<sub>5</sub>-H), 10.32, 10.39 (1H, s, CONH, exch.). <sup>13</sup>C NMR (DMSO-d<sub>6</sub>) δ: 18.38 (COCH<sub>3</sub>), 22.61 (CH<sub>3</sub>CHCH<sub>3</sub>), 22.64 (CH<sub>3</sub>CHCH<sub>3</sub>), 30.08 (CH<sub>3</sub>CHCH<sub>3</sub>), 35.46 (NCH<sub>3</sub>), 42.66 (COCH<sub>3</sub>), 42.76 (CH<sub>2</sub>), 79.89 (NCHN), 112.58 (ArCH), 114.78 (ArCH), 118.23 (ArCH), 126.99 (ArCH), 127.51 (ArCH), 128.43 (ArCH), 128.98 (ArCH), 129.16 (ArCH), 129.55 (ArCH), 135.01 (ArC), 137.36 (ArC), 138.56 (ArC), 139.83 (ArC), 147.38 (ArC), 160.89 (ArC), 172.77 (ArC). MS, m/z: 442 (M<sup>+</sup>). Analysis calcd. for C<sub>28</sub>H<sub>31</sub>N<sub>3</sub>O<sub>2</sub>: C, 76.16; H, 7.08; N, 9.52. Found: C, 75.77; H, 7.01; N, 9.30.

### 2.1.9. *N*-(2-(4-chlorophenyl)-1-methyl-4-oxo-1,4-dihydroquinazolin-3(2H)-yl)-2-(4-isobutylphenyl) propenamide (7b)

White crystals, yield 77%, m.p. 120–125 °C.  $^1\text{H NMR}$  (DMSO- $d_6$ )  $\delta$ : 0.88 (6H, d,  $J=5.6$ ,  $\text{CH}_3\text{CHCH}_3$ ), 1.34 (3H, d,  $J=7$ ,  $\text{CH}_3\text{CHCO}$ ), 1.83–1.86 (1H, m,  $\text{CH}_3\text{CHCH}_3$ ), 2.45 (2H, d,  $J=7.12$ ,  $\text{CHCH}_2$ ), 2.71 (3H, s, NCH<sub>3</sub>), 3.65 (1H, q,  $J=7.04$ ,  $\text{CH}_3\text{CHCO}$ ), 5.65 (1H, s, NCHN), 6.73 (1H, d,  $J=8.32$ , quinazolinone-C<sub>8</sub>-H), 6.87 (1H, t,  $J=7.4$ , quinazolinone-C<sub>6</sub>-H), 7.05 (2H, d,  $J=8.4$ , phenyl-C<sub>2,6</sub>-H), 7.11 (2H, d,  $J=8$ , ibuprofen phenyl-C<sub>3,5</sub>-H), 7.17 (2H, d,  $J=8.04$ , ibuprofen phenyl-C<sub>2,6</sub>-H), 7.31 (2H, d,  $J=8.4$ , phenyl-C<sub>3,5</sub>-H), 7.45 (1H, t,  $J=7.12$ , quinazolinone-C<sub>7</sub>-H), 7.79 (1H, d,  $J=6.32$ , quinazolinone-C<sub>5</sub>-H), 10.31 (1H, s, CONH, exch.).  $^{13}\text{C NMR}$  (DMSO- $d_6$ )  $\delta$ : 18.44 (COCH<sub>3</sub>), 22.64 ( $\text{CH}_3\text{CHCH}_3$ ), 22.67 ( $\text{CH}_3\text{CHCH}_3$ ), 30.12 ( $\text{CH}_3\text{CHCH}_3$ ), 35.36 (NCH<sub>3</sub>), 42.81 (COCHCH<sub>3</sub>), 44.72 (CH<sub>2</sub>), 79.18 (NCHN), 112.77 (ArCH), 114.78 (ArCH), 118.42 (ArCH), 127.50 (ArCH), 128.51 (ArCH), 128.96 (ArCH), 128.99 (ArCH), 129.29 (ArCH), 134.13 (ArC), 135.13 (ArC), 136.40 (ArC), 138.83 (ArC), 139.93 (ArC), 147.27 (ArC), 160.84 (ArC), 172.73 (ArC). **MS**,  $m/z$ : 476 (M<sup>+</sup>), 478 (M<sup>+</sup>). Analysis calcd. for C<sub>28</sub>H<sub>30</sub>ClN<sub>3</sub>O<sub>2</sub>: C, 70.65; H, 6.35; N, 8.83. Found: C, 70.38; H, 6.26; N, 8.46.

### 2.1.10. 2-(4-Isobutylphenyl)-*N*-(1-methyl-2-(4-nitrophenyl)-4-oxo-1,4-dihydroquinazolin-3(2H)-yl) propenamide (7c)

Yellow powder, yield 72%, m.p. 111–116 °C.  $^1\text{H NMR}$  (DMSO- $d_6$ )  $\delta$ : 0.88 (6H, d,  $J=1.84$ ,  $\text{CH}_3\text{CHCH}_3$ ), 1.33 (3H, d,  $J=7$ ,  $\text{CH}_3\text{CHCO}$ ), 1.81–1.85 (1H, m,  $\text{CH}_3\text{CHCH}_3$ ), 2.43 (2H, d,  $J=7$ ,  $\text{CHCH}_2$ ), 2.75 (3H, s, NCH<sub>3</sub>), 3.63 (1H, q,  $J=7.04$ ,  $\text{CH}_3\text{CHCO}$ ), 5.86 (1H, s, NCHN), 6.67 (1H, d,  $J=8.32$ , quinazolinone-C<sub>8</sub>-H), 6.89 (1H, t,  $J=7.44$ , quinazolinone-C<sub>6</sub>-H), 7.68 (2H, d,  $J=$  ibuprofen phenyl-C<sub>3,5</sub>-H), 7.16 (2H, d,  $J=8.12$ , ibuprofen phenyl-C<sub>2,6</sub>-H), 7.34 (2H, d,  $J=8.68$ , phenyl-C<sub>2,6</sub>-H), 7.48 (1H, t,  $J=7.04$ , quinazolinone-C<sub>7</sub>-H), 7.81 (1H, d,  $J=6.32$ , quinazolinone-C<sub>5</sub>-H), 8.09 (2H, d,  $J=8.68$ , phenyl-C<sub>3,5</sub>-H), 10.36 (1H, s, CONH, exch.).  $^{13}\text{C NMR}$  (DMSO- $d_6$ )  $\delta$ : 18.47 (COCH<sub>3</sub>), 22.58 ( $\text{CH}_3\text{CHCH}_3$ ), 22.63 ( $\text{CH}_3\text{CHCH}_3$ ), 30.09 ( $\text{CH}_3\text{CHCH}_3$ ), 35.49 (NCH<sub>3</sub>), 42.91 (COCHCH<sub>3</sub>), 44.67 (CH<sub>2</sub>), 78.96 (NCHN), 113.08 (ArCH), 114.80 (ArCH), 118.84 (ArCH), 124.07 (ArCH), 127.53 (ArCH), 128.61 (ArCH), 129.17 (ArCH), 129.28 (ArCH), 135.30 (ArC), 138.71 (ArC), 139.99 (ArC), 144.39 (ArC), 147.19 (ArC), 148.25 (ArC), 160.94 (ArC), 172.91 (ArC). **MS**,  $m/z$ : 486 (M<sup>+</sup>). Analysis calcd. for C<sub>28</sub>H<sub>30</sub>N<sub>4</sub>O<sub>4</sub>: C, 69.12; H, 6.21; N, 11.51. Found: C, 69.33; H, 6.03; N, 11.30.

### 2.1.11. 2-(4-Isobutylphenyl)-*N*-(2-(4-methoxyphenyl)-1-methyl-4-oxo-1,4-dihydroquinazolin-3(2H)-yl) propenamide (7d)

Brown powder, yield 30%, m.p. 92–95 °C.  $^1\text{H NMR}$  (DMSO- $d_6$ )  $\delta$ : 0.88 (6H, d,  $J=6.52$ ,  $\text{CH}_3\text{CHCH}_3$ ), 1.34 (3H, d,  $J=6.84$ ,  $\text{CH}_3\text{CHCO}$ ), 1.83–1.86 (1H, m,  $\text{CH}_3\text{CHCH}_3$ ), 2.44 (2H, d,  $J=7.04$ ,  $\text{CHCH}_2$ ), 2.68 (3H, s, NCH<sub>3</sub>), 3.65–3.74 (4H, m, OCH<sub>3</sub>,  $\text{CH}_3\text{CHCO}$ ), 5.53 (1H, s, NCHN), 6.71 (1H, d,  $J=8.32$ , quinazolinone-C<sub>8</sub>-H), 6.77 (2H, d,  $J=7.64$ , phenyl-C<sub>3,5</sub>-H), 6.84 (1H, t,  $J=7.48$ , quinazolinone-C<sub>6</sub>-H), 6.92 (2H, d,  $J=7.6$ , phenyl-C<sub>2,6</sub>-H), 7.11 (2H, d,  $J=7.48$ , ibuprofen phenyl-C<sub>3,5</sub>-H), 7.18 (2H, d,  $J=7.24$ , ibuprofen phenyl-C<sub>2,6</sub>-H), 7.43 (1H, t,  $J=7.84$ , quinazolinone-C<sub>7</sub>-H), 7.78 (1H, d,  $J=7.64$ , quinazolinone-C<sub>5</sub>-H), 10.27 (1H, s, CONH, exch.).  $^{13}\text{C NMR}$  (DMSO- $d_6$ )  $\delta$ : 18.44 (COCH<sub>3</sub>), 22.63 ( $\text{CH}_3\text{CHCH}_3$ ), 22.68 ( $\text{CH}_3\text{CHCH}_3$ ), 30.14 ( $\text{CH}_3\text{CHCH}_3$ ), 35.32 (NCH<sub>3</sub>), 42.72 (COCHCH<sub>3</sub>), 44.72 (CH<sub>2</sub>), 55.54 (OCH<sub>3</sub>), 79.51 (NCHN), 112.55 (ArCH), 114.25 (ArCH), 114.84 (ArCH), 118.08 (ArCH), 124.07 (ArCH), 127.52 (ArCH), 128.39 (ArCH), 129.29 (ArCH), 129.51 (ArC), 134.99 (ArC), 138.95 (ArC), 139.88 (ArC), 147.44 (ArC), 160.16 (ArC), 160.89 (ArC), 172.64 (ArC). **MS**,  $m/z$ : 472 (M<sup>+</sup>).

Analysis calcd. for C<sub>29</sub>H<sub>33</sub>N<sub>3</sub>O<sub>3</sub>: C, 73.86; H, 7.05; N, 8.91. Found: C, 74.01; H, 6.85; N, 8.58.

### 2.1.12. *N*-(2-(4-fluorophenyl)-1-methyl-4-oxo-1,4-dihydroquinazolin-3(2H)-yl)-2-(4-isobutylphenyl) propenamide (7e)

Yellowish brown powder, yield 35%, m.p. 90–95 °C.  $^1\text{H NMR}$  (DMSO- $d_6$ )  $\delta$ : 0.88 (6H, d,  $J=6.4$ ,  $\text{CH}_3\text{CHCH}_3$ ), 1.34 (3H, d,  $J=7.04$ ,  $\text{CH}_3\text{CHCO}$ ), 1.82–1.86 (1H, m,  $\text{CH}_3\text{CHCH}_3$ ), 2.44 (2H, d,  $J=7.12$ ,  $\text{CHCH}_2$ ), 2.70 (3H, s, NCH<sub>3</sub>), 3.65 (1H, q,  $J=7.04$ ,  $\text{CH}_3\text{CHCO}$ ), 5.63 (1H, s, NCHN), 6.73 (1H, d,  $J=8.28$ , quinazolinone-C<sub>8</sub>-H), 6.86 (1H, t,  $J=7.44$ , quinazolinone-C<sub>6</sub>-H), 7.06–7.11 (6H, m, phenyl-C<sub>2,6</sub>-H, ibuprofen phenyl-C<sub>3,5</sub>-H, phenyl-C<sub>3,5</sub>-H), 7.17 (2H, d,  $J=8.04$ , ibuprofen phenyl-C<sub>2,6</sub>-H), 7.54 (1H, t,  $J=7.08$ , quinazolinone-C<sub>7</sub>-H), 7.79 (1H, d,  $J=6.28$ , quinazolinone-C<sub>5</sub>-H), 10.29 (1H, s, CONH, exch.).  $^{13}\text{C NMR}$  (DMSO- $d_6$ )  $\delta$ : 18.41 (COCH<sub>3</sub>), 22.62 ( $\text{CH}_3\text{CHCH}_3$ ), 22.65 ( $\text{CH}_3\text{CHCH}_3$ ), 30.12 ( $\text{CH}_3\text{CHCH}_3$ ), 35.33 (NCH<sub>3</sub>), 42.80 (COCHCH<sub>3</sub>), 44.70 (CH<sub>2</sub>), 79.20 (NCHN), 112.74 (ArCH), 114.77 (ArCH), 115.67 (d,  $J=22$ , ArCH), 118.37 (ArCH), 127.50 (ArCH), 128.50 (ArCH), 129.29 (ArCH), 129.32 (d,  $J=8$ , ArCH), 133.73 (d,  $J=3$ , ArC), 135.14 (ArC), 138.82 (ArC), 139.95 (ArC), 147.32 (ArC), 160.90 (ArC), 164.06 (d,  $J=245.5$ , ArC), 172.75 (ArC). **MS**,  $m/z$ : 459 (M<sup>+</sup>), 461 (M<sup>+</sup>). Analysis calcd. for C<sub>28</sub>H<sub>30</sub>FN<sub>3</sub>O<sub>2</sub>: C, 73.18; H, 6.58; N, 9.14. Found: C, 73.13; H, 6.43; N, 8.95.

### 2.1.13. Method for synthesis of ethyl 2-((4-oxo-3-(benzamido)-3,4-dihydroquinazolin-2-yl)thio)acetate (12a), and ethyl 2-((4-oxo-3-(2-phenylacetamido)-3,4-dihydroquinazolin-2-yl)thio)acetate (12b)

A mixture of compounds (**11a**, **b**, 0.01 mole) were mixed with anhydrous K<sub>2</sub>CO<sub>3</sub> (4 g, 0.03 mole) and ethyl chloro acetate (1.84 g, 0.015 mole) in anhydrous acetone (25 ml) and stirred at 30 °C for 4–8 h<sup>29</sup>. The mixture was filtered and acetone distilled off. The remaining precipitates were stirred with distilled H<sub>2</sub>O, filtered and dried to be used in the next step without further purification.

### 2.1.14. *N*-(2-mercapto-4-oxoquinazolin-3(4H)-yl)-2-phenylacetamide (11b)

White powder, yield 70%, m.p. 279–280 °C.  $^1\text{H NMR}$  (DMSO- $d_6$ )  $\delta$ : 3.69 (2H, q,  $J=14.8$ , CH<sub>2</sub>), 7.26 (1H, t,  $J=7.2$ , phenyl-C<sub>4</sub>-H), 7.34 (2H, t,  $J=7.28$ , phenyl-C<sub>3,5</sub>-H), 7.38–7.44 (4H, m, phenyl-C<sub>2,6</sub>-H, quinazolinone-C<sub>8,6</sub>-H), 7.80 (1H, t,  $J=7.80$ , quinazolinone-C<sub>7</sub>-H), 7.98 (1H, d,  $J=6.8$ , quinazolinone-C<sub>5</sub>-H), 11.17 (1H, s, CONH, exch.), 13.16 (1H, s, CSNH, exch.)<sup>28</sup>.

### 2.1.15. Ethyl 2-((4-oxo-3-(2-phenylacetamido)-3,4-dihydroquinazolin-2-yl)thio)acetate (12b)

White powder, yield 84%, m.p. 107–108 °C.  $^1\text{H NMR}$  (DMSO- $d_6$ )  $\delta$ : 1.23 (3H, t,  $J=7.08$ , CH<sub>3</sub>), 3.77 (2H, s, COCH<sub>2</sub>), 4.01 (2H, s, S-CH<sub>2</sub>), 4.15 (2H, q,  $J=7.04$ , CH<sub>2</sub>CH<sub>3</sub>), 7.29 (1H, m, phenyl-C<sub>4</sub>-H), 7.38 (4H, m, phenyl-C<sub>2,6</sub>-H), 7.51 (2H, t,  $J=5.48$ , quinazolinone-C<sub>6,8</sub>-H), 7.85 (1H, t,  $J=6.96$ , quinazolinone-C<sub>7</sub>-H), 8.09 (1H, d,  $J=6.96$ , quinazolinone-C<sub>5</sub>-H), 11.49 (1H, s, CONH, exch.).

### 2.1.16. General method of preparing *N*-(2-((2-hydrazinyl-2-oxoethyl)thio)-4-oxoquinazolin-3(4H)-yl) benzamide (13a), and *N*-(2-((2-hydrazinyl-2-oxoethyl)thio)-4-oxoquinazolin-3(4H)-yl) 2-phenylacetamide (13b)

A mixture of ethyl ester for compounds (**12a**, **b**, 4 g, 0.01 mole), and hydrazine hydrate (1.5 g, 0.03 mole) in absolute ethanol

(20 ml) was stirred at 30 °C for 12 h. The white precipitates formed were filtered, washed with distilled H<sub>2</sub>O and dried off to give the pure target compounds without further purification.

#### 2.1.17. *N*-2-((2-hydrazinyl-2-oxoethyl)thio)-4-oxoquinazolin-3(4H)-yl benzamide (13a)

white powder, yield 87%, m.p. 208–213 °C. <sup>1</sup>H NMR (DMSO-d<sub>6</sub>) δ: 3.83 (1H, d, *J* = 14.44, SCH), 3.96 (1H, d, *J* = 14.44, SCH), 4.34 (2H, bs, NH<sub>2</sub>, exch.), 7.54 (1H, t, *J* 7.76, quinazolinone-C<sub>6</sub>-H), 7.61–7.72 (4H, m, benzoyl-C<sub>3,5</sub>, 4-H, quinazolinone-C<sub>8</sub>-H), 7.88 (1H, t, *J* = 6.44, quinazolinone-C<sub>7</sub>-H), 8.00 (2H, d, *J* = 7.28, benzoyl-C<sub>2,6</sub>-H), 8.11 (1H, d, *J* = 7.88, quinazolinone-C<sub>5</sub>-H), 9.38 (1H, s, CONH, exch.), 11.15 (1H, bs, CONH, exch.). <sup>13</sup>C NMR (DMSO-d<sub>6</sub>) δ 33.95 (SCH<sub>2</sub>), 119.74 (ArCH), 126.86 (ArCH), 126.90 (ArCH), 127.14 (ArCH), 128.32 (ArCH), 129.37 (ArCH), 131.47 (ArCH), 133.50 (ArC), 135.87 (ArC), 147.15 (ArC), 158.92 (ArC), 159.12 (ArC), 166.32 (ArC), 166.74 (ArC). **MS**, *m/z*: 370 (M<sup>+</sup>). Analysis calcd. for C<sub>17</sub>H<sub>15</sub>N<sub>5</sub>O<sub>3</sub>S: C, 55.28; H, 4.09; N, 18.96. Found: C, 55.14; H, 4.03; N, 18.76.

#### 2.1.18. *N*-2-((2-hydrazinyl-2-oxoethyl)thio)-4-oxoquinazolin-3(4H)-yl-2-phenylacetamide (13b)

white powder, yield 83%, m.p. 210–215 °C. <sup>1</sup>H NMR (DMSO-d<sub>6</sub>) δ: 3.78 (3H, d, *J* = 17.24, COCH<sub>2</sub> + SCH), 3.89 (1H, d, *J* = 14.56, SCH), 4.32 (2H, bs, NH<sub>2</sub>, exch.), 7.30 (1H, m, phenyl-C<sub>4</sub>-H), 7.34–7.40 (4H, m, phenyl -C<sub>2,6</sub>, 3,5-H), 7.5 (1H, t, *J* = 7.28, quinazolinone-C<sub>6</sub>-H), 7.62 (1H, d, *J* = 8.08, quinazolinone-C<sub>8</sub>-H), 7.85 (1H, t, *J* = 7.04, quinazolinone-C<sub>7</sub>-H), 8.08 (1H, d, *J* = 7, quinazolinone-C<sub>5</sub>-H), 9.36 (1H, s, CONH, exch.), 11.23 (1H, bs, CONH, exch.). <sup>13</sup>C NMR (DMSO-d<sub>6</sub>) δ 33.89 (SCH<sub>2</sub>), 119.67 (ArCH), 126.78 (ArCH), 126.83 (ArCH), 127.10 (ArCH), 127.29 (ArCH), 128.84 (ArCH), 129.76 (ArCH), 134.90 (ArC), 135.79 (ArC), 147.05 (ArC), 158.72 (ArC), 158.85 (ArC), 166.77 (ArC), 170.55 (ArC). <sup>13</sup>C NMR (Pyridine-d<sub>6</sub>) δ 34.48 (SCH<sub>2</sub>), 41.15 (CH<sub>2</sub>), 120.26 (ArCH), 125.86 (ArCH), 126.55 (ArCH), 127.03 (ArCH), 127.09 (ArCH), 128.68 (ArCH), 129.82 (ArCH), 134.69 (ArC), 134.82 (ArC), 147.40 (ArC), 159.12 (ArC), 159.34 (ArC), 167.96 (ArC), 171.21 (ArC). **MS**, *m/z*: 383(M<sup>+</sup>). Analysis calcd. for C<sub>18</sub>H<sub>17</sub>N<sub>5</sub>O<sub>3</sub>S: C, 56.39; H, 4.47; N, 18.27. Found: C, 56.53; H, 4.43; N, 18.47.

#### 2.1.19. General method for preparation of *N*-2-((2-(4-substitutedbenzoyl) hydrazinyl)-2-oxoethyl)thio)-4-oxoquinazolin-3(4H)-yl-(2-phenylacetamide) or (benzamide) (14a-d)

The titled compounds were prepared as in the reported method<sup>30</sup> with some modification as following: A mixture of substituted hydrazides compounds (**13a,b**, 1 g, 0.003 mole) and liquid benzoyl chloride derivatives (0.01 mole) were mixed using glass rod, then I<sub>2</sub> pellets were added (0.1 g, 0.0003 mole) with continuous mixing for 5 min under fume cupboard. The brown semisolids formed were vigorously washed with saturated solutions of sodium thio-sulphate, followed by adding sodium bicarbonate and stirring up to 5 h at 40 °C. The precipitates were filtered, washed with brine H<sub>2</sub>O then with petroleum ether and left to dry to give the desired pure compounds (**14a-d**)

#### 2.1.20. *N*-2-((2-(2-benzoylhydrazinyl)-2-oxoethyl)thio)-4-oxoquinazolin-3(4H)-ylbenzamide (14a)

white powder, yield 78%, m.p. 194–198 °C. <sup>1</sup>H NMR (DMSO-d<sub>6</sub>) δ 4.03 (1H, d, *J* = 15, SCH), 4.12 (1H, d, *J* = 15, SCH), 7.48–7.65 (6H, m, benzoyl-C<sub>3,5</sub>, 4-H, benzoyl-C<sub>3,5</sub>, 4-H), 7.71 (1H, t, *J* = 7.4, quinazolinone -C<sub>6</sub>-H), 7.78 (1H, d, *J* = 8.08, quinazolinone-C<sub>8</sub>-H),

7.87–7.92 (3H, m, benzoyl-C<sub>2,6</sub>-H, quinazolinone-C<sub>7</sub>-H), 8.01 (2H, d, *J* = 7.2, benzoyl-C<sub>2,6</sub>-H), 8.12 (1H, d, *J* = 6.96, quinazolinone-C<sub>5</sub>-H), 10.40 (1H, s, CONH, exch.), 10.51 (1H, s, CONH, exch.), 11.87 (1H, s, CONH, exch.). <sup>13</sup>C NMR (DMSO-d<sub>6</sub>) δ 33.83 (SCH<sub>2</sub>), 119.75 (ArCH), 126.90 (ArCH), 127.10 (ArCH), 127.16 (ArCH), 127.94 (ArCH), 128.32 (ArCH), 128.92 (ArCH), 129.39 (ArCH), 131.43 (ArCH), 132.32 (ArCH), 132.82 (ArC), 133.53 (ArC), 135.85 (ArC), 147.19 (ArC), 158.87 (ArC), 158.94 (ArC), 165.82 (ArC), 166.33 (ArC), 166.83 (ArC). **MS**, *m/z*: 474 (M<sup>+</sup>). Analysis calcd. for C<sub>24</sub>H<sub>19</sub>N<sub>5</sub>O<sub>4</sub>S: C, 60.88; H, 4.04; N, 14.79. Found: C, 60.60; H, 3.82; N, 15.06.

#### 2.1.21. *N*-2-((2-(2-(4-chlorobenzoyl)hydrazinyl)-2-oxoethyl)thio)-4-oxoquinazolin-3(4H)-ylbenzamide (14b)

white powder, yield 90%, m.p. 215–220 °C. <sup>1</sup>H NMR (DMSO-d<sub>6</sub>) δ: 4.07 (2H, q, *J* = 14.92, SCH<sub>2</sub>), 7.53–7.79 (7H, m, benzoyl-C<sub>3,5</sub>, 4-H, chloro benzoyl-C<sub>3,5</sub>-H, quinazolinone-C<sub>6</sub>, 8-H), 7.89–7.94 (3H, m, benzoyl-C<sub>2,6</sub>-H, quinazolinone-C<sub>7</sub>-H), 8.01 (2H, d, *J* = 7.36, chloro benzoyl-C<sub>2,6</sub>-H), 8.13 (1H, d, *J* = 7.8, quinazolinone-C<sub>5</sub>-H), 10.44 (1H, s, CONH, exch.), 10.61 (1H, s, CONH, exch.), 11.87 (1H, s, CONH, exch.). <sup>13</sup>C NMR (DMSO-d<sub>6</sub>) δ: 33.79 (SCH<sub>2</sub>), 119.74 (ArCH), 126.89 (ArCH), 127.09 (ArCH), 127.15 (ArCH), 128.33 (ArCH), 129.09 (ArCH), 129.18 (ArCH), 129.38 (ArCH), 129.88 (ArCH), 131.52 (ArC), 133.50 (ArC), 135.82 (ArC), 137.20 (ArC), 147.18 (ArC), 158.86 (ArC), 158.95 (ArC), 164.86 (ArC), 166.40 (ArC), 166.89 (ArC). **MS**, *m/z*: 507 (M<sup>+</sup>), 509 (M<sup>+</sup> + 2). Analysis calcd. for C<sub>24</sub>H<sub>18</sub>ClN<sub>5</sub>O<sub>4</sub>S: C, 56.75; H, 3.57; N, 13.79. Found: C, 56.64; H, 3.66; N, 14.00.

#### 2.1.22. *N*-2-((2-(2-benzoylhydrazinyl)-2-oxoethyl)thio)-4-oxoquinazolin-3(4H)-yl-2-phenylacetamide (14c)

white powder, yield 99%, m.p. 235–240 °C. <sup>1</sup>H NMR (DMSO-d<sub>6</sub>) δ: 3.77 (2H, s, COCH<sub>2</sub>), 3.98 (1H, d, *J* = 15, SCH), 4.10 (1H, d, *J* = 15, SCH), 7.27–7.31 (1H, m, phenyl C<sub>4</sub>-H), 7.35–7.41 (4H, m, phenyl C<sub>2,6</sub>, 3,5-H), 7.48–7.53 (3H, m, benzoyl C<sub>4,3,5</sub>-H), 7.58 (1H, t, *J* = 7.32, quinazolinone C<sub>6</sub>-H), 7.74 (1H, d, *J* = 8.04, quinazolinone C<sub>8</sub>-H), 7.86–7.89 (3H, m, quinazolinone C<sub>7</sub>-H, benzoyl C<sub>2,6</sub>-H), 8.09 (1H, d, *J* = 7.88, quinazolinone C<sub>5</sub>-H), 10.38 (1H, s, CONH, exch.), 10.51 (1H, s, CONH, exch.), 11.49 (1H, s, CONH, exch.). <sup>13</sup>C NMR (DMSO-d<sub>6</sub>) δ 33.81 (SCH<sub>2</sub>), 41.15 (CH<sub>2</sub>), 119.68 (ArCH), 126.83 (ArCH), 127.11 (ArCH), 127.31 (ArCH), 127.93 (ArCH), 128.71 (ArCH), 128.95 (ArCH), 129.47 (ArCH), 129.77 (ArCH), 132.36 (ArCH), 132.77, (ArC), 134.91 (ArC), 135.78 (ArC), 147.10 (ArC), 158.59 (ArC), 158.75 (ArC), 165.86 (ArC), 166.89 (ArC), 170.61 (ArC). **MS**, *m/z*: 487 (M<sup>+</sup>). Analysis calcd. for C<sub>25</sub>H<sub>21</sub>N<sub>5</sub>O<sub>4</sub>S: C, 61.59; H, 4.34; N, 14.37. Found: C, 61.56; H, 4.30; N, 14.38.

#### 2.1.23. *N*-2-((2-(2-(4-chlorobenzoyl)hydrazinyl)-2-oxoethyl)thio)-4-oxoquinazolin-3(4H)-yl-2-phenylacetamide (14d)

White powder, yield 98%, m.p. 221–226 °C. <sup>1</sup>H NMR (DMSO-d<sub>6</sub>) δ: 3.78 (2H, s, CH<sub>2</sub>), 4.07 (2H, q, *J* = 27.44, SCH<sub>2</sub>), 7.28 (1H, t, *J* = 6.76, phenyl-C<sub>4</sub>-H), 7.35–7.41 (4H, m, phenyl-C<sub>2,6</sub>, 3,5-H), 7.51 (1H, t, *J* = 7.56, quinazolinone-C<sub>6</sub>-H), 7.58 (2H, d, *J* = 8.28, benzoyl-C<sub>3,5</sub>-H), 7.73 (1H, d, *J* = 8.12, quinazolinone-C<sub>8</sub>-H), 7.86–7.92 (3H, m, quinazolinone-C<sub>7</sub>-H, benzoyl-C<sub>2,6</sub>-H), 8.08 (1H, d, *J* = 7.88, quinazolinone-C<sub>5</sub>-H), 10.44 (1H, s, CONH, exch.), 10.63 (1H, s, CONH, exch.), 11.57 (1H, s, CONH, exch.). <sup>13</sup>C NMR (DMSO-d<sub>6</sub>) δ: 33.80 (SCH<sub>2</sub>), 119.69 (ArCH), 126.80 (ArCH), 127.11 (ArCH), 127.27 (ArCH), 128.83 (ArCH), 129.07 (ArCH), 129.15 (ArCH), 129.79 (ArCH), 129.91 (ArCH), 131.54 (ArC), 134.99 (ArC), 135.74 (ArC), 137.16 (ArC), 147.09 (ArC), 158.63 (ArC), 158.70 (ArC), 164.81 (ArC), 166.85 (ArC), 170.59 (ArC). **MS**, *m/z*: 522 (M<sup>+</sup>), 524 (M<sup>+</sup> + 2). Analysis calcd. for

C<sub>25</sub>H<sub>20</sub>CIN<sub>5</sub>O<sub>4</sub>S: C, 57.53; H, 3.86; N, 13.42. Found: C, 57.77; H, 3.58; N, 13.49.

#### 2.1.24. The unexpected new compound *N*-(4-oxoquinazolin-3(4*H*)-yl)-2-phenylacetamide (IV):

White crystalline powder, yield 40%, m.p. 277–280 °C. <sup>1</sup>H NMR (DMSO-*d*<sub>6</sub>) δ: 3.75 (2H, *s*, CH<sub>2</sub>), 5.85 (1H, *s*, NCHN), 7.28 (1H, *t*, *J* = 6.76, phenyl- C<sub>4</sub>-H), 7.35–7.40 (4H, *m*, phenyl-C<sub>2,6</sub>, <sub>3,5</sub>-H), 7.52 (1H, *t*, *J* = 7.72, quinazolinone-C<sub>6</sub>-H), 7.86 (1H, *t*, *J* = 7.2, quinazolinone-C<sub>7</sub>-H), 8.12 (1H, *d*, *J* = 6.48, quinazolinone C<sub>8</sub>-H), 8.94 (1H, *d*, *J* = 8.48, quinazolinone-C<sub>5</sub>-H), 11.23 (1H, *s*, CONH, *exch*).

## 2.2. Biological activity

### 2.2.1. In vitro COX-1 and COX-2 inhibitory assay

All the newly synthesised compounds were tested for their ability to inhibit COX-1 and COX-2 enzymes using a screening assay method. The colorimetric ovine COX-1/human recombinant COX-2 assay Kit (catalogue No. 560131, Cayman Chemicals Inc., Ann Arbor, MI, USA) was used according to the supplier's instructions and previously reported studies<sup>12,31,32</sup>

The IC<sub>50</sub> of inhibition of COX-1/COX-2 activities in three replicates was calculated and is presented as the average of three values ± SEM (*n* = 3). The standards: Celecoxib, ibuprofen, indomethacin, and diclofenac were used as reference drugs in the study, and the SI values were calculated as IC<sub>50</sub> (COX-1)/IC<sub>50</sub> (COX-2).

### 2.2.2. Experimental animals

Adult male Wistar rats (200–250 g) were purchased from the Faculty of Veterinary Medicine, Zagazig (Egypt) and kept in the animal house facility at the Pharmacology Department, Faculty of Pharmacy, Zagazig University (Egypt) for one week before starting the experiments under standard conditions of light/dark cycle and 23–25 °C. Animals had free access to standard laboratory chow and water (*ad libitum*). All the experimental protocols were approved by the ethical committee at Zagazig University (ECAHZU), Faculty of Pharmacy, Zagazig University, Egypt, with a registration number (P15-12-2017) and are in accordance with the National Institutes of Health Guide for the Care and Use of Laboratory Animals 8th Edition<sup>33</sup>.

**2.2.2.1. In vivo anti-inflammatory assay.** Carrageenan-induced rat paw oedema test was used to investigate the anti-inflammatory activity of the selected compounds (**4a**, **b**, **7c**, **13b**, and **14c**) as previously reported<sup>13,14,34,35</sup>.

The rats were divided into nine groups (*n* = 5/group). All tested compounds were suspended in 1% Tween-80. Group 1, controls, were given the vehicle (1% Tween80, 10 ml/kg). The remaining groups each received one of the selected compounds (50 mg/kg) or one of the three reference drugs ibuprofen (20 mg/kg), indomethacin (20 mg/kg) or celecoxib (50 mg/kg). The rats were given the drugs 1 h before the injection of carrageenan solution (1% in 0.9% NaCl, 0.1 ml) (Sigma Aldrich, USA) in the sub-planter tissue of the right hind paw. The paw thickness (mm) was measured using a calliper before (0 h) and after carrageenan injection at 1, 2, 3, 4, 5 and 24 h. The inhibition of oedema thickness was calculated using the following formula (control– drug/control) × 100.

**2.2.2.2. Gastric acute ulcerogenic activity.** The selected compounds (**4a**, **b**, **7c**, **13b**, **14c**) were evaluated for their ulcerogenic

activity in rats, using the high ulcerogenic indomethacin and low ulcerogenic celecoxib as references. The rats from the previous experiment were fasted for 12 h., followed by the administration of additional doses of the selected compounds or the two references for two consecutive days. Six hrs after the last treatment, the animals were sacrificed, and their stomachs were removed, washed with saline solution (0.9%) and examined for ulceration using a magnifying lens. The ulcer scores were estimated according to the method prescribed by Kulkarni and as detailed in our previous studies<sup>36–38</sup>. The following scores were individually assigned to each lesion: normal coloured stomach, 0; red colouration, 0.5; spot ulcers, 1; haemorrhagic streaks, 1.5; ulcer >3 but <5 mm, 2; and ulcers >5 mm, 3.

The ulcer index (UI) was calculated according to the following equation:

$$[UI = UN + US + UP \times 10^{-1}],$$

where UN, US and UP are the ulcers number, severity score, and the percentage of animals with an ulcer, respectively.

### 2.2.2.3. In vivo analgesic assay: acetic acid induced writhing test.

The analgesic activity of the selected 5 compounds was measured using acetic acid-induced writhing pain model as previously reported<sup>39</sup> using celecoxib as reference drug. Briefly, mice were divided into 7 groups (*n* = 5/group) that received either the vehicle (1% Tween 80, 10 ml/kg), the tested compounds (**4a**, **b**, **7c**, **13b**, and **14c**) (50 mg/kg, *p.o*) or celecoxib (50 mg/kg, *p.o*) 1 h prior acetic acid injection (0.7%, 1 ml/100 g, *i.p*). The number of writhes, manifested as extension of hind legs, constriction of abdomen, or turning of trunk was recorded within 30 min.

### 2.2.3. Cell culture studies

Human colorectal cancer cell lines, HCT116 and HT29, and RAW 264.7 macrophages were obtained from ATCC (Manassas, VA). HCA7 colorectal cancer cell line was obtained from Sigma. HT29 and HCT116 cells were cultured in McCoy's 5A medium (Sigma Aldrich, St. Louis, MO) containing 10% heat-inactivated foetal bovine serum (HI-FBS) (Gibco, USA), 100 μg/mL streptomycin (Invitrogen, USA), and 100 mg/ml penicillin (Invitrogen, USA)<sup>40</sup>. HCA7 and RAW 264.7 cells were cultured in Dulbecco's minimal essential media (DMEM, Invitrogen) containing 10% HI-FBS, sodium pyruvate (1 mM), penicillin (100 mg/mL), and streptomycin (100 mg/m)<sup>41,42</sup>.

#### 2.2.3.1. NO production in LPS-activated RAW 264.7 macrophages.

NO was measured using 4-amino-5-methylamino-2,7-difluorofluorescein diacetate (DAF-FM diacetate; Molecular Probes, USA). Briefly, RAW 264.7 cells were cultured in black 96-well plates (200,000 cells/mL, 100 μl/well) for 24 h. The cells were incubated with the individual test compounds or the reference drugs at different concentrations (6.5, 12.5, 25, 50, and 100 μM) for 2 h. at 37 °C followed by the incubation with LPS at a final concentration of 1 μg/mL for additional 20 h.<sup>43</sup> The assay was then performed by washing the cells with phosphate-buffered saline (PBS) and incubating with 2 μM 2',7'-dichlorofluorescein diacetate (DAF-FM) in serum-free medium. The fluorescence intensity, which is directly proportional to NO levels, was quantified, as detailed in our previous study<sup>44</sup>. IC<sub>50</sub> values were calculated from the dose–response curves.

#### 2.2.3.2. ROS production in LPS-activated RAW 264.7 macrophages.

The general probe of oxidative species 2,7-dichlorofluorescein

diacetate (DCFH-DA) (Molecular Probes), was used to investigate the antioxidant potential of the test compounds following the induction of inflammation in RAW 264.7 by LPS. The cells were cultured, incubated with the different test compounds, and activated with LPS (1  $\mu\text{g}/\text{mL}$ ) as detailed above. The cells were then incubated with DCFH-DA (25  $\mu\text{M}$ ) and the fluorescence intensity, which is directly proportional to intracellular ROS levels was measured as detailed in our previous report<sup>44</sup>.  $\text{IC}_{50}$  values were calculated from the dose–response curves.

**2.2.3.3. MTS cell viability assays.** Cells were cultured in 96-well plates for 48 h and then treated with serum-free media containing different concentrations of the tested compounds (12.5, 25, 50, 100 and 150  $\mu\text{M}$ ). After 48 h., MTS reagent (Promega) was added as directed by the manufacturer, and then, the absorbance was measured at 495 nm. The absorbance is proportional to the number of viable cells.  $\text{IC}_{50}$  was calculated from the dose-response curves as described previously<sup>45</sup> using GraphPad Prism 8 software (GraphPad Software, San Diego, CA).

### 2.3. Molecular docking and in silico study

#### 2.3.1. Docking study

Molecular docking of the selected compounds (**4a,b**, **7c**, **13b**, and **14c**) was performed to provide insight on their binding efficiencies with the active sites of COX-1 and COX-2. The molecular modelling studies of the compounds 2D, and 3D were carried out using Molecular Operating Environment MOE version 2018 software (Chemical Computing Group, Montreal, CA). The X-ray crystallographic complex structures of Cyclooxygenase-2 enzyme (COX-2) with ligand SC-558 (PDB entry 1CX2), and Cyclooxygenase-1 enzyme (COX-1) with ibuprofen (PDB code 1EQG) were downloaded from protein data bank website (<http://www.rcsb.org>). We used ibuprofen and SC-558 as references and both were redocked for validation. The protein structures were prepared after deletion of  $\text{H}_2\text{O}$  molecules, repeated chains, and unwanted surfactants. Hydrogen atoms and partial charges were added using MOE quick preparation tool. Final compound data were prepared by adding hydrogen atoms, calculating partial charges, and minimising energy (MMF94). The docking poses were selected according to the best scoring functions.

#### 2.3.2. In silico prediction of pharmacokinetic and physicochemical properties

Compounds (**4a**, **b**, **7c**, **13b**, and **14c**) were subjected to screening assays for drug likeness and water solubility, Lipinski's rule of five for drug Topological polar surface area (TPSA), oral bioavailability, toxicity and other pharmacokinetic by three software: Molinspiration Chemoinformatics server<sup>46</sup>, PreADMET calculator<sup>47</sup> and the OSIRIS Property Explorer<sup>48</sup>. The resulting parameters were used to predict the *in vivo* behaviour of synthesised drugs compared with reference drugs. The values of TPSA are used to calculate the percentage of oral absorption (%ABS) using the following equation:  $\%ABS = 109 - 0.345 \text{TPSA}^{49}$ .

Osiris property explorer<sup>48</sup> an online portal by Thomas Sander, Idorsia Pharmaceuticals Ltd, that provides predictions about the toxicity of any organic compound using a two-colour indicator; properties with a high degree of undesired effects are shown in red, whereas a green colour indicates drug-conforming behaviour.

### 2.4. Statistical analysis

The data were analysed using Graph Pad Prism 8 software (GraphPad Software, San Diego, CA, USA). One-way analysis of variance (ANOVA) or repeated-measures analysis of variance (RM-ANOVA) followed by Tukey's *post hoc* test were used to state significance between groups. Data are presented as the mean  $\pm$  SEM. Differences were considered significant at  $p < 0.05$ .

## 3. Results and discussion

### 3.1. Chemistry

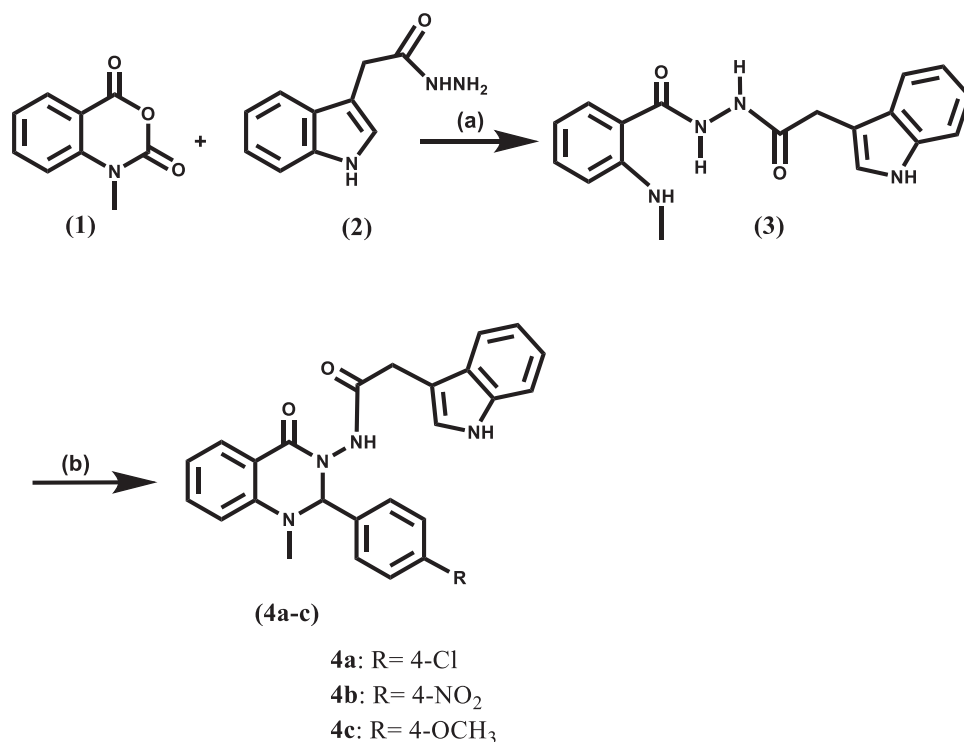
Two new series of hybrid bioactive molecules of 2,3 dihydroquinazolin-4(1H)-one with either indole-3- acetic acid or ibuprofen moiety were prepared using Schemes 1 and 2. We altered our hybrid construction of 2,3 dihydroquinazolin-4(1H) one with indole moiety instead of indomethacin upon experiencing difficulties in the preparation of indomethacin hydrazide via hydrazinolysis of its methyl ester. It was reported that this hydrazinolysis resulted in debenzoylation of indomethacin instead of formation of indomethacin hydrazide as illustrated in (Figure 2)<sup>50</sup>. The plethora of reported COX inhibitory activities associated with many indole derivatives<sup>15–18</sup> encouraged us to utilise 2-(1H-indole-3-yl) acetohydrazide. This compound was prepared from indole-3-acetic acid as an alternative to indomethacin hydrazide.

To incorporate a bioactive anti-inflammatory moiety (either indomethacin-alternative or ibuprofen, respectively), as the aryl ring attached to position 3 of the quinazolinone scaffold, the N-methyl-isatoic anhydride (**1**) was used as the starting material in the preparation of benzohydrazide derivatives (**3** and **6**) of the two series. Through condensation reactions with either 2-(1H-indole-3-yl) acetohydrazide or (R/S) 2–4-isobutyl phenyl propanehydrazide, the intermediates **3** and **6** were synthesised. The chemical structure of intermediate **3** was investigated by <sup>1</sup>H NMR to reveal four NH signals at  $\delta = 9.97$  (CONH), 10.06 (CONH), and 10.89 (Indole NH) ppm that are exchangeable by  $\text{D}_2\text{O}$ . Similarly, the chemical structural investigation of intermediate **6** was identified by <sup>1</sup>H NMR to indicate the presence of three NH singlet signals at  $\delta = 7.45$  (NHCH<sub>3</sub>), 9.97 (CONH), and 10.05 ppm (CONH) exchangeable with  $\text{D}_2\text{O}$ , in addition to the presence of <sup>1</sup>H NMR isobutyl profile;  $\delta = 0.87$  (6H, d, CH<sub>3</sub>CHCH<sub>3</sub>), 1.79–1.84 (1H, m, CH<sub>3</sub>CHCH<sub>3</sub>), and 2.42 (2H, d, CHCH<sub>2</sub>–C<sub>6</sub>H<sub>4</sub>–).

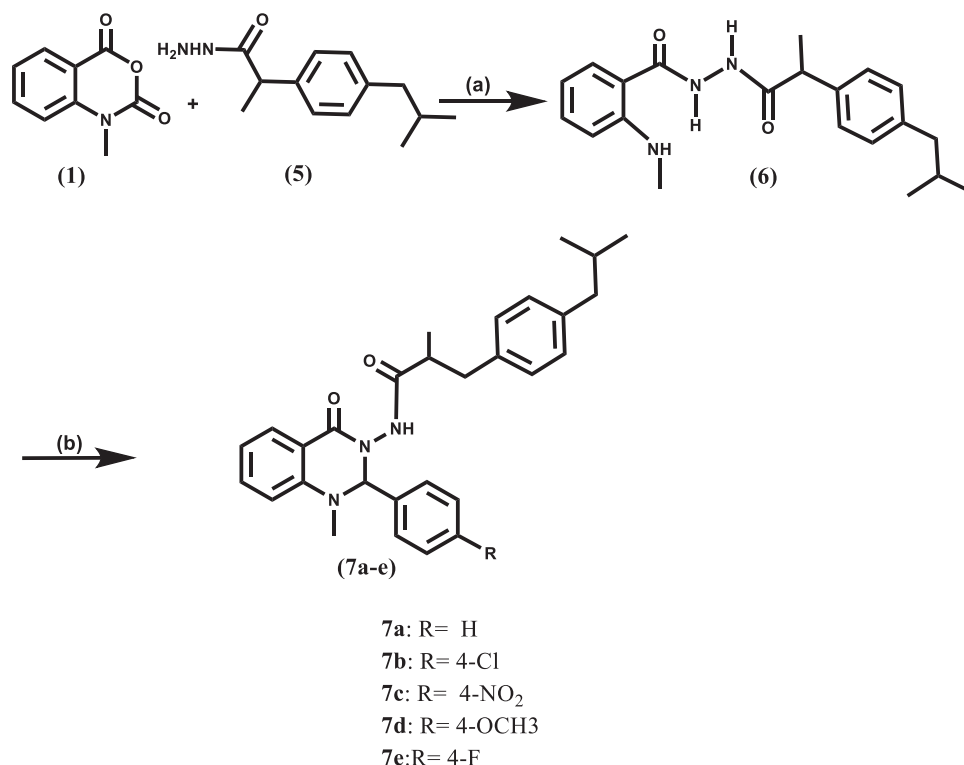
To maintain the 2,3 diaryl-heterocyclic moiety (V-shape) of the final target bioactive compounds N-(2-(4-substitutedphenyl)-1-methyl-4-oxo-1,4-dihydroquinazolin-3(2H)-yl)-2-(1H-indol-3-yl) acetamide (**4a-c**) in Scheme 1 and N-(2-(4-substitutedphenyl)-1-methyl-4-oxo-1,4-dihydroquinazolin-3(2H)-yl)-2-(4-isobutylphenyl) propenamide (**7a-e**) in Scheme 2, cyclisation of the intermediates (**3** and **6**) was carried out using aromatic aldehydes in glacial acetic acid. The chemical structures of the final compounds **4a-c** were confirmed by <sup>1</sup>H NMR, <sup>13</sup>C NMR, mass spectra and elemental analysis. Using these methods, <sup>1</sup>H NMR spectra indicated the cyclisation of the intermediate benzohydrazide (**3**) to 2,3 dihydroquinazolin-4 (1H)-one derivatives (**4a-c**), as only two NH signals presented in each of the final compounds representing CONH and indole NH, respectively, at  $\delta = 10.43$ , 10.90 (**4a**), 10.48, 10.89 (**4b**), and 10.39, 10.89 (**4c**) ppm. Additionally, the benzylic proton singlet signal for (**4a-c**) was at  $\delta = 5.78$ , 5.96, and 5.68 ppm, respectively. Moreover, <sup>13</sup>C NMR spectra revealed the presence of the characteristic C2-quinazoline carbon (NCHN) signal for (**4a-c**) at  $\delta = 79.37$ , 79.06, and 79.74 ppm, respectively.

The chemical structures of the final compounds (**7a-e**) were identified by <sup>1</sup>H NMR, <sup>13</sup>C NMR, mass spectra, and elemental





**Scheme 1.** Synthetic route of target compounds, reagent, and conditions: (a) C<sub>2</sub>H<sub>5</sub>OH/2 ml glacial acetic acid, reflux, 12 h; (b) Appropriate aromatic aldehyde, glacial acetic acid, or C<sub>2</sub>H<sub>5</sub>OH/2 ml glacial acetic acid, reflux, 8–24 h.

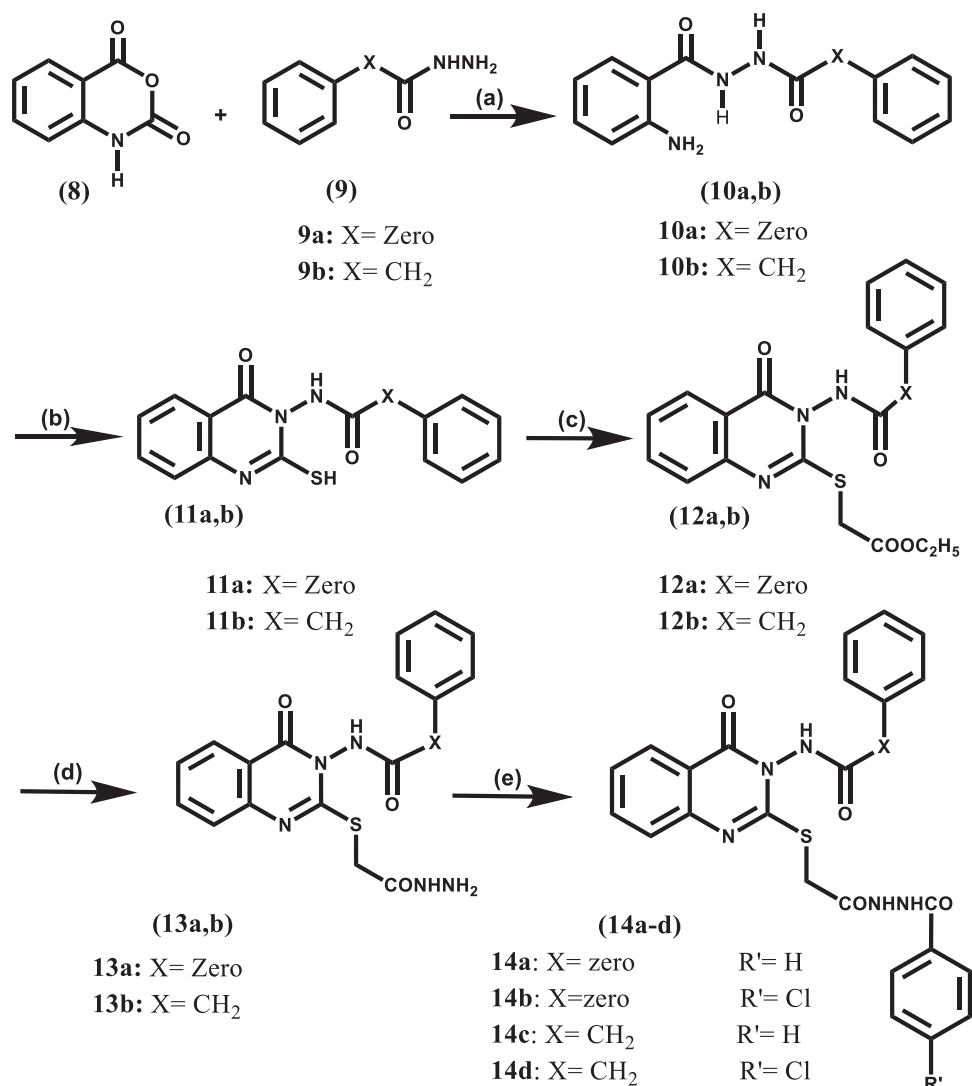


**Scheme 2.** Synthetic route of target compounds, reagent, and conditions: (a) C<sub>2</sub>H<sub>5</sub>OH/2 ml glacial acetic acid, reflux, 3 h; (b) Appropriate aromatic aldehyde, glacial acetic acid, reflux, 8 h.

analysis. The <sup>1</sup>H NMR spectra of these hybrids revealed the restriction of three NH signals of the intermediate **6** at  $\delta = \text{---}t$  R spectra and 10.05 ppm to one NH signal of the final targets (**7a-e**) at  $\delta \approx 10.30$  ppm with the benzylic proton appearing as a sharp singlet signal at  $\delta \approx 5.60$  ppm. In addition to <sup>1</sup>H NMR spectra of these

compounds (**7a-e**) included the isobutyl profile. Moreover, <sup>13</sup>C NMR spectra revealed the presence of the characteristic C2-quinazoline carbon (NCHN) signal for (**7a-e**) at  $\delta \approx 79$  ppm.

In **Scheme 3**, the starting material was isatoic anhydride (**8**) which was condensed with either benzoic acid hydrazide or



**Scheme 3.** Synthetic route of target compounds, reagent, and conditions: (a) C<sub>2</sub>H<sub>5</sub>OH, 2 ml acetic acid, reflux, 8 h; (b) 2 equivalent KOH, excess CS<sub>2</sub>, 95% C<sub>2</sub>H<sub>5</sub>OH, reflux, 48 h; (c) Ethyl chloroacetate, 2 equivalent k<sub>2</sub>CO<sub>3</sub>, Anhydrous Acetone, rt, stirr, 3–8 h; (d) N<sub>2</sub>H<sub>4</sub>·H<sub>2</sub>O, C<sub>2</sub>H<sub>5</sub>OH, rt, stirr, 12 h; (e) 3.5 equivalent liquid benzoyl chloride derivatives, stirr, 1 equivalent (I<sub>2</sub>) pellets, wash Na thiosulphate sat.sol, NaHCO<sub>3</sub> sat.sol, Brine sat.sol.

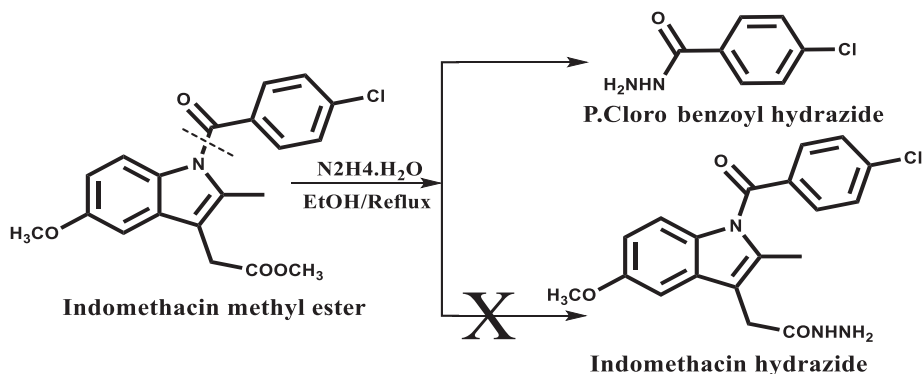


**Figure 2.** Illustrate the cleavage of indomethacin ester in hydrazinolysis<sup>50</sup>.

phenyl acetohydrazide to study the introduction of flexibility between the quinazolinone scaffold and the aryl moiety at position 3, producing benzohydrazide intermediates (**10 a, b**). Adding sulphur bridge at position 2 of the quinazolinone moiety was achieved by condensation of benzohydrazide intermediates (**10 a, b**) with CS<sub>2</sub> in the presence of alcoholic KOH then acid neutralisation to give intermediates (**11a, b**) which were identified by their

reported melting points<sup>27,28</sup>. The synthesis of intermediates (**12a, b**) was performed by alkylation of 2-mercapto-4(3H) quinazolinone derivatives (**11a, b**) with ethyl chloroacetate in anhydrous acetone. The final hydrazides (**13a, b**) that incorporated the targeted thioacetohydrazide linker were obtained by hydrazinolysis of the ester (**12a, b**) in mild conditions. We found that heating even as low as 40 °C led to the breakdown of the sulphur bridge and

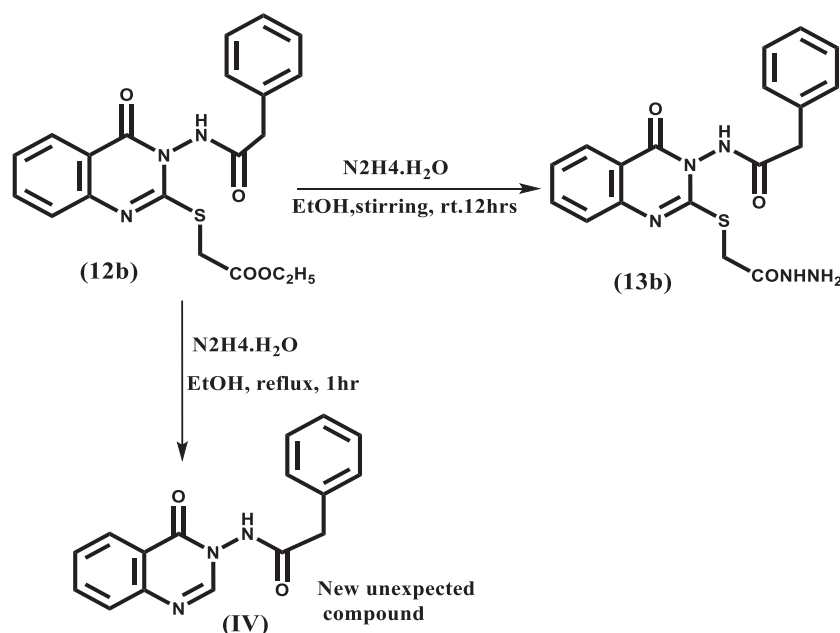


Figure 3. Different compounds for **12b** resulted according to change in conditions.

gave the unexpected compound **IV** as shown in the (Figure 3); its chemical structure was identified by  $^1\text{H}$  NMR (Supplementary data).

The  $^1\text{H}$  NMR spectra of compounds (**13a,b**) revealed the absence of triplet–quartette of ethyl group of the esters (**12a,b**) and the presence of three NH signals at  $\delta = 4.34$  (2H,  $\text{NH}_2$ ), 9.38 (1H, CONH), and 11.15 ppm (1H, CONH) for compound **13a** and at  $\delta = 4.32$  (2H,  $\text{NH}_2$ ), 9.36 (1H, CONH), and 11.23 (1H, CONH) for compound **13b**.  $^{13}\text{C}$  NMR spectrum of compound **13a** revealed the presence of the  $\text{SCH}_2$  signal at  $\delta = 33.95$  ppm while that of compound **13b** showed the  $\text{SCH}_2$  signal at  $\delta = 34.48$  ppm in addition to  $\text{CH}_2$  of phenylacetamide signal at  $\delta = 41.15$  ppm.

To maintain the 2,3 diaryl-heterocyclic moiety (V-shape), the final series N-(2-((2-(2-(4-substitutedbenzoyl) hydrazinyl)-2-oxoethyl) thio)-4-oxoquinazolin-3(4H)-yl) benzamide (XVIIa, b) and N-(2-((2-(2-(4-substitutedbenzoyl) hydrazinyl)-2-oxoethyl)thio)-4-oxoquinazolin-3(4H)yl)2phenylacetamide (**14a-d**) was formed by benzoylation of hydrazides (**13a, b**) using the catalytic acylation of amino compounds in presence of  $\text{I}_2$  as catalyst<sup>30</sup>.

The  $^1\text{H}$  NMR spectra of the final compounds (**14a-d**) indicates the absence of amino group signal from the hydrazides (**13a,b**) and the appearance of three amidic NH signals at  $\delta = 10.40$ , 10.51, and 11.87 ppm for (**14a**), 10.44, 10.61, and 11.87 for (**14b**), 10.38, 10.51, and 11.49 ppm for (**14c**) and 10.44, 10.63, and 11.57 ppm for (**14d**).

## 3.2. Biological activity

### 3.2.1. In vitro COX-1 and COX-2 inhibitory assay

All the final compounds (**4a-c**, **7a-e**, **13a,b** and **14a-d**) were tested in comparison with indomethacin, ibuprofen, and celecoxib as reference drugs (Table 1). The efficacies of our compounds was evaluated by estimating the half-maximal inhibitory concentration ( $\text{IC}_{50}$ ) and the selectivity index (SI) values calculated as  $\text{IC}_{50}(\text{COX-1})/\text{IC}_{50}(\text{COX-2})$ .

The incorporation of a bioactive anti-inflammatory moiety (either indomethacin-like (compounds **4a,c**) or ibuprofen (compounds **7a-e**) to position 3 of the quinazolinone scaffold, as well

Table 1. In vitro COX-1/COX-2 inhibition assay

Compound Code	<sup>a</sup> COX-1 $\mu\text{M}$ $\text{IC}_{50}$	<sup>a</sup> COX-2 $\mu\text{M}$ $\text{IC}_{50}$	<sup>b</sup> Selectivity Index (SI)
Celecoxib	14.75 $\pm$ 0.15	0.04 $\pm$ 0.20	368.78
Indomethacin	0.09 $\pm$ 0.13	0.71 $\pm$ 0.15	0.13
Ibuprofen	4.13 $\pm$ 0.08	1.67 $\pm$ 0.25	2.47
<b>4a</b>	12.68 $\pm$ 0.11	0.04 $\pm$ 0.08	317.00
<b>4b</b>	6.93 $\pm$ 0.15	0.07 $\pm$ 0.22	99.00
<b>4c</b>	11.21 $\pm$ 0.13	0.03 $\pm$ 0.33	373.67
<b>7a</b>	12.76 $\pm$ 0.10	0.05 $\pm$ 0.13	255.02
<b>7b</b>	13.35 $\pm$ 0.10	0.04 $\pm$ 0.13	333.75
<b>7c</b>	14.73 $\pm$ 0.13	0.037 $\pm$ 0.20	398.11
<b>7d</b>	14.37 $\pm$ 0.16	0.04 $\pm$ 0.25	359.25
<b>7e</b>	11.85 $\pm$ 0.15	0.04 $\pm$ 0.23	296.25
<b>13a</b>	10.19 $\pm$ 0.14	0.04 $\pm$ 0.18	254.75
<b>13b</b>	16.92 $\pm$ 0.16	0.045 $\pm$ 0.18	373.77
<b>14a</b>	10.86 $\pm$ 0.20	0.03 $\pm$ 0.17	362.00
<b>14b</b>	12.98 $\pm$ 0.12	0.04 $\pm$ 0.29	324.5
<b>14c</b>	15.44 $\pm$ 0.17	0.04 $\pm$ 0.33	359.74
<b>14d</b>	12.56 $\pm$ 0.11	0.04 $\pm$ 0.38	314.00

<sup>a</sup> $\text{IC}_{50}$  in ( $\mu\text{M}$ ) concentration as expressed as mean  $\pm$  SEM, for three replications.

<sup>b</sup>Selectivity index =  $(\text{COX-1 } \text{IC}_{50}/\text{COX-2 } \text{IC}_{50})$ .

as the incorporation of a thioacetohydrazide linker at position 2 of the quinazolinone moiety (compounds **13a,b** and **14a-d**), not only succeeded in making our new compounds exhibit superior potency and selectivity towards COX-2 (SI = 254–398) over previously reported quinazolinones (**1**)<sup>13</sup> (SI = 38.63–99.67), but also showed nearly the same COX-1 and COX-2 inhibitory activities (COX-1  $\text{IC}_{50}$  = 10.19–16.92 and COX-2  $\text{IC}_{50}$  = 0.03–0.05  $\mu\text{M}$ ) as that of celecoxib. Excitingly, the SI values of the new compounds are comparable to that of celecoxib (SI = 368.75) with the exception of compound **4b** which has relatively lower COX-2 selectivity (SI = 99, COX-1  $\text{IC}_{50}$  = 6.93  $\mu\text{M}$ , COX-2  $\text{IC}_{50}$  = 0.07  $\mu\text{M}$ ).

For Scheme 1: compounds (**4a,c**) of indole bioactive molecule showed SI values (SI = 373–317) that are several-fold higher than that of indomethacin (SI = 0.13) and nearly the same as that of celecoxib. The difference in the *para* substituent of the phenyl ring attached to position 2 of the quinazolinone in this series caused a dramatic change in COX-1 inhibitory activity, as the *para* nitro derivative (**4b**) showed a significantly greater potency (2-

fold) towards COX-1 than compounds (**4a,c**) carrying *para* Cl or OCH<sub>3</sub>, respectively. The latter modification resulted in a decrease in **4b** selectivity index (SI = 99.00) which is superior to that of indomethacin.

For Scheme 2: series (**7a-e**) of ibuprofen bioactive molecule showed SI (SI = 255–398) of approximately 150-fold greater than that of ibuprofen (SI = 2.47) and nearly the same as that of celecoxib. Conversely to the indole series (**4a-c**), no significant change in COXs inhibitory activity was observed upon alternating the *para* substituent of the phenyl ring attached to position 2 of the quinazolinone. Importantly, the *para* nitro derivative (**7c**) showed slight improvement in SI value (SI = 398.11) compared to that of celecoxib (SI = 368.75).

For Scheme 3: Thioacetohydrazide containing series (**13a,b-14a-d**), all compounds showed SI values (SI = 254–373) that are nearly equal or slightly higher than that of celecoxib. Introducing a degree of flexibility between the quinazolinone scaffold and the aryl moiety at position 3 led to an improvement in the SI. Compounds with phenyl acetamide moiety (X = CH<sub>2</sub>) (**13b** and **14c,d**) showed better SI values compared with their benzamide counterparts (**13a** and **14a,b**). This difference may also be due to the increase in their sizes to reduce COX-1 affinity.

In general, increasing the overall bulkiness of the quinazolinone scaffold either at position 3 (compounds **4a-c** and **7a-e**) or position 2 (compounds **13a,b** and **14a-d**) enhanced COX-2 inhibition activity and selectivity for COX-1. This may contribute to the larger size of the COX-2 active site and/or the ability of the inserted extension (indole-like, ibuprofen or thioacetohydrazide) to engage in additional intermolecular interactions within COX-2 active site.

Ibuprofen was better than indomethacin compounds. The incorporated bioactive anti-inflammatory moiety with COX-2 selectivity in the ibuprofen containing compounds **7b,c** (with Cl (SI = 333) and NO<sub>2</sub> (SI = 398)) showed superior SI values compared to their indomethacin-like containing counterparts **4a,b** (with Cl (SI = 317), with NO<sub>2</sub> (SI = 99)).

Both based on these favourable results and in order to limit animal use, we chose five compounds **4a,b**, **7c**, **13b**, and **14c** for further *in vivo* investigation. Each of these compounds chosen represents those with the best SI in each series; **4b** showed the lowest SI among all the synthesised compounds and was included for comparison. The potential ability to limit the production of nitric oxide (NO) and reactive oxygen species (ROS) as well as to identify anticancer activity was investigated *in vitro* using RAW 264.7 macrophages and colorectal cancer cell lines, respectively.

### 3.2.2. *In vivo* anti-inflammatory assay

The carrageenan-induced rat paw oedema assay was used to test the anti-inflammatory activity of the selected compounds (**4a,b**,

**7c**, and **13b**, **14c**). Table 2 showed that the percent of inhibition of oedema for compounds **4b** (with indomethacin-like moiety), **7c** (with ibuprofen moiety) and **13b** (with thioacetohydrazide moiety) was nearly the same as that of celecoxib (47.60%) and ibuprofen (47.18%), and greater than that of indomethacin (33.81%). The greatest percent inhibition was 49.47% for compound **4b** which has the indole ring as bioactive molecule and nitro group in the *para* position. The other indole derivative (**4a**) with a *para* chloro group achieved 33.40% inhibition of oedema, which was similar to that of indomethacin (33.81% inhibition) and lower than that of celecoxib (47.60% inhibition).

The two compounds **4b** and **7c** with *para* nitro substitution as bulk electron withdrawing group seems to have enhanced activity (nearly the same as celecoxib, 47.60% oedema inhibition) than that of compounds **4a** and **14c** with a *para* chloro or no substitution, respectively. In contrast to COX-2 selectivity, the percent of inhibition of oedema was slightly improved by incorporating an indomethacin-alternative entity as an active moiety (**4b**, 49.47%) rather than incorporating ibuprofen one (**7c**, 45.37%).

For the class of thioacetohydrazides, the addition of phenyl ring in compound **14c** decreased the *in vivo* anti-inflammatory activity more than that of compound **13b** which lacks the phenyl ring (31.86% vs. 45.49% oedema inhibition).

### 3.2.3. Acute gastric ulcerogenic activity

All the tested compounds (**4a,b**, **7c**, **13b**, and **14c**) had better ulcer index (UI) (3 – 8.26), than that of the reference compounds indomethacin (23.8) and ibuprofen (15). Compound **4a** that has the indole ring as bioactive molecule and a *para* chloro substitution, and an UI of 3 which is similar to the value of the reference drug celecoxib (2.4) (Table 3)

### 3.2.4. *In vivo* analgesic assay: Acetic acid-induced writhing test

The analgesic activity for the selected compounds (**4a,b**, **7c**, **13b**, and **14c**) was evaluated using the acetic acid-induced writhing test using celecoxib as a positive control. The efficacy of the tested compounds as analgesic were measured by their ability to attenuate acetic acid-induced abdominal writhing. Notably, all the tested compounds showed better analgesic activity (range 0 – 21.75 writhes) than that of celecoxib (29.20 writhes) (Figure 4).

Interestingly, the thioacetohydrazide containing **13b** showed exceptional analgesic activity as it was able to completely abolish the pain response with no writhes followed by compound **7c** (11.33 writhes), which has the ibuprofen as bioactive molecule and nitro group in *para* position, and showed 78% reduction in the pain response (writhes number).

**Table 2.** *In vivo* anti-inflammatory activity in carrageenan-induced paw oedema in rat.

Tested compounds	Mean oedema thickness (mm) ± SEM							Average oedema inhibition%
	0h	1h	2h	3h	4h	5h	24h	
Control	0.00 ± 0.00	2.98 ± 0.09	3.66 ± 0.02	2.90 ± 0.18	2.71 ± 0.17	2.79 ± 0.12	0.96 ± 0.10	–
4a	0.00 ± 0.00	2.67 ± 0.24	2.90 ± 0.33*	2.14 ± 0.25	2.04 ± 0.24	1.39 ± 0.06*	0.54 ± 0.21	33.40
4b	0.00 ± 0.00	1.39 ± 0.09*	1.89 ± 0.25*	1.70 ± 0.17*	1.14 ± 0.22*	1.42 ± 0.28*	0.16 ± 0.08	49.47
7c	0.00 ± 0.00	1.79 ± 0.04*	2.21 ± 0.35*	1.90 ± 0.44*	1.62 ± 0.26*	1.55 ± 0.29	0.06 ± 0.04	45.37
13b	0.00 ± 0.00	2.26 ± 0.30	2.58 ± 0.41*	2.67 ± 0.15	1.97 ± 0.29	1.61 ± 0.23*	0.45 ± 0.14	45.49
14c	0.00 ± 0.00	3.02 ± 0.35	2.89 ± 0.13*	2.42 ± 0.18	2.37 ± 0.19	2.34 ± 0.23	0.57 ± 0.09	31.86
Indomethacin	0.00 ± 0.00	2.00 ± 0.14*	2.21 ± 0.12*	1.82 ± 0.13*	2.02 ± 0.16	1.87 ± 0.18*	0.49 ± 0.10	33.81
Ibuprofen	0.00 ± 0.00	1.76 ± 0.07*	2.00 ± 0.15*	1.74 ± 0.08*	1.23 ± 0.16*	1.36 ± 0.18*	0.48 ± 0.15	47.18
Celecoxib	0.00 ± 0.00	1.27 ± 0.07*	1.51 ± 0.07*	1.49 ± 0.14*	1.39 ± 0.12*	1.19 ± 0.08*	0.53 ± 0.12	47.60

The thickness of paw oedema was measured at before (0) and 1, 2, 3, 4, 5 and 24 h. after the induction of inflammation. Data are mean ± SEM. The percentage inhibition of oedema thickness was calculated for each compound using the area under the curve of all time points (n = 5). \*p < 0.05, significantly different from control.

**Table 3.** Acute ulcerogenicity activity.

Compounds	Number of rats with ulcer	Lesion Incidence (%)	Average Ulcer number	Ulcer Index (UI) <sup>a</sup>
Control	0	0	0	Nil
<b>4a</b>	3	60	1.6	8.26
<b>4b</b>	1	20	0.8	3
<b>7c</b>	3	60	1	8
<b>13b</b>	2	40	0.4	4.8
<b>14c</b>	2	40	0.8	5.3
Indomethacin	5	100	12.4	23.8
Ibuprofen	5	100	3.8	15
Celecoxib	1	20	0.2	2.4

<sup>a</sup>The ulcer index (UI) was calculated according to the equation: (UI = UN + US + UPX10<sup>-1</sup>), (n = 5).

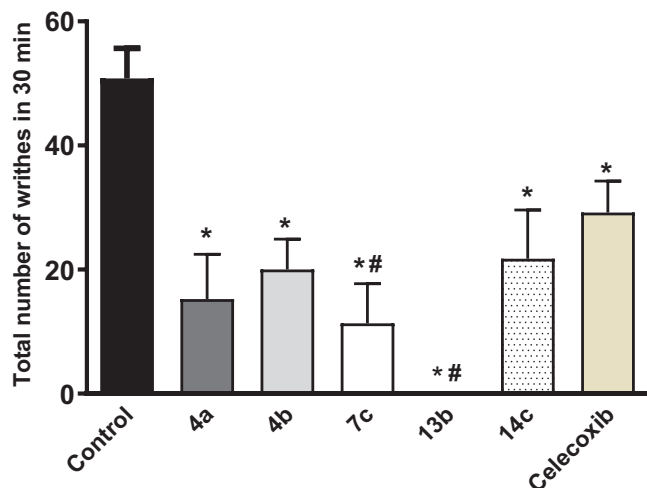


**Figure 4.** Effect of the tested compounds (50 mg/kg, p.o.) and celecoxib (50 mg/kg, p.o) on acetic acid-induced writhing in mice. Statistical analysis was performed using one way ANOVA followed by Tukey's *post hoc* test. Data is expressed as mean  $\pm$  SEM (n = 5). \**p* < 0.05 vs. control values. #*p* < 0.05 vs. celecoxib.

**Table 4.** *In vitro* NO and ROS production:

Compound	NO IC <sub>50</sub> ( $\mu$ M)	ROS IC <sub>50</sub> ( $\mu$ M)
<b>4a</b>	31.46 $\pm$ 1.08	29.67 $\pm$ 1.07
<b>4b</b>	32.16 $\pm$ 1.316	24.46 $\pm$ 2.06
<b>7c</b>	23.41 $\pm$ 1.29	9.228 $\pm$ 1.76
<b>13b</b>	9.76 $\pm$ 2.14	24.37 $\pm$ 1.43
<b>14c</b>	12.98 $\pm$ 1.36	16.18 $\pm$ 1.30
Celecoxib	19.51 $\pm$ 1.11	11.75 $\pm$ 1.11
Ibuprofen	18.77 $\pm$ 1.19	36.43 $\pm$ 1.45
Indomethacin	25.28 $\pm$ 1.01	68.92 $\pm$ 1.29

NO: nitric oxide; ROS: reactive oxygen species.

Ibuprofen was favoured to indomethacin-like as the incorporated bioactive anti-inflammatory moiety to attenuate the abdominal pain as the ibuprofen conjugate **7c** showed better analgesic activity than its indomethacin-like conjugated counterparts **4a,b**. Similarly, the addition of phenyl ring in the thioacetohydrazide **14c** decreased the analgesic activity more than compound **13b** which lacks the phenyl ring.

### 3.2.5. Effects on NO and ROS production in LPS-activated RAW 264.7 macrophages cells

Lipopolysaccharides (LPS)-activated RAW 264.7 macrophage cells are a widely used *in vitro* model to study different inflammatory responses and to screen the mechanism of action of new anti-inflammatory candidates. Exposure of RAW 264.7 cells to the

bacterial toxin LPS triggers a strong inflammatory status with the release of a number of inflammatory mediators including COX-2<sup>43</sup>. LPS also induces nitric oxide (NO) production by upregulating the inducible isoform of nitric oxide synthase which is required to maintain prolonged COX-2 expression<sup>51</sup>. Reactive oxygen species (ROS) are highly involved in the inflammatory response including LPS-mediated inflammation and can induce the production of a myriad of inflammatory cytokines<sup>52</sup>. Numerous *in vivo* and *in vitro* studies have shown that compounds with antioxidant potential are effective as anti-inflammatory and anti-cancer drugs<sup>52–54</sup>. All the tested compounds (**4a,b**, **7c**, **13b**, and **14c**) inhibited the production of the inflammatory mediator NO with IC<sub>50</sub> = 9.76 – 32.16  $\mu$ M with some compounds having an effect that was greater than that of indomethacin (IC<sub>50</sub> = 25.28  $\mu$ M). The two compounds with a thioacetohydrazide bridge **13b** and **14c** (IC<sub>50</sub> = 9.76 and 12.98  $\mu$ M, respectively) showed superior scores compared to the three reference drugs celecoxib, ibuprofen, and indomethacin (IC<sub>50</sub> = 19.51, 18.77 and 25.28, respectively). The two compounds with an indole bioactive molecule (**4a**, **b**) showed approximately 1.3-fold better IC<sub>50</sub> values than that of indomethacin. The compound (**7c**) that was conjugated with ibuprofen as bioactive molecule showed IC<sub>50</sub> of 23.41  $\mu$ M which is slightly higher than that of ibuprofen (IC<sub>50</sub> = 18.77  $\mu$ M) (Table 4).

All the selected compounds (**4a,b**, **7c**, **13b**, and **14c**) inhibited ROS production with IC<sub>50</sub> = 9.23 – 29.67  $\mu$ M, indicating improved antioxidant activity compared with the two reference compounds ibuprofen (IC<sub>50</sub> = 36.43  $\mu$ M) and indomethacin (IC<sub>50</sub> = 68.92  $\mu$ M). The most potent compound in reducing ROS levels was the ibuprofen-containing compound **7c** that showed an IC<sub>50</sub> value, which was lower than that of celecoxib (9.22 vs. 11.75  $\mu$ M) and of the thioacetohydrazide-containing compound **14c** with IC<sub>50</sub> of 16.18  $\mu$ M (Table 4). Notably, none of the tested concentrations were toxic to RAW 264.7 macrophages as tested by MTS cell bio-availability assay.

Again, incorporating ibuprofen as an active moiety was favoured to an indomethacin-alternative one in reducing both NO and ROS levels. The ibuprofen conjugate **7c** was the most potent in reducing both NO and ROS levels compared with its indomethacin-like conjugated counterparts **4a,b**.

### 3.2.6. MTS Cell viability assays

NSAIDs of highly selective cyclooxygenase COX-2 inhibitory activity were proven by numerous experimental, epidemiologic, and clinical studies to be promising candidates as anticancer agents. COX-2 activity and expression are increased in colorectal cancer; NSAIDs, which inhibit COX-2 activity, could have the potential to inhibit colorectal carcinogenesis<sup>55,56</sup>. In order to explore the anticancer potential of the tested compounds owing to their COX-2 inhibition activity, we performed *in vitro* anticancer activity evaluation of the 5 tested compounds (**4a,b**, **7c**, **13b**, and **14c**) against three colon cancer cell lines that express different levels of COX-2: The HT29 cell line, which moderately expresses COX-2, the HCT116 cell line, which lacks COX-2 expression, and the HCA7 cell line, which expresses high levels of COX-2<sup>57</sup>.

Compound **4a** has an indole ring as its bioactive molecule and a *para* chloro substitution and was the only compound that showed anticancer efficacy in all three tested cell lines HCT116, HT29 and HCA7 with IC<sub>50</sub> values of 75.35, 15.42, and 137.3  $\mu$ M, respectively. Interestingly, the active anticancer compounds **4a**, **4b** (indole conjugates), and **7c** (ibuprofen conjugate) showed their maximal effect in the HT29 cell line which moderately expresses COX-2 with IC<sub>50</sub> values of 15.42, 66.67, and 13.42  $\mu$ M,

**Table 5.** Cell viability assays

Compound	*HCT116 IC <sub>50</sub> (μM)	*HT29 IC <sub>50</sub> (μM)	*HCA7 IC <sub>50</sub> (μM)
<b>4a</b>	75.35 ± 0.10	15.42 ± 0.06	137.3 ± 0.08
<b>4b</b>	>150	66.67 ± 0.07	>150
<b>7c</b>	>150	13.42 ± 0.17	>150
<b>13b</b>	>150	>150	>150
<b>14c</b>	>150	>150	>150
Celecoxib	53.77 ± 0.05	5.82 ± 0.38	51.36 ± 0.04

\* (HCT116), \*(HT29), \*(HCA7) are colon cancer cell lines that either scarcely, moderately or highly express COX-2, respectively.

respectively, indicating their effectiveness as COX-2 inhibitors (Table 5). As expected, all the tested compounds have relatively low cytotoxic activity against HCT116 cell line, which lacks COX-2 expression. Additionally, only compound **4a** was able to achieve a cytotoxic effect at concentrations less than 150 μM (IC<sub>50</sub> = 137.3 μM) in HCA7 cell line, having high levels of COX-2 expression. This finding could be explained by the relatively high concentrations required to overcome high COX-2 activity in this particular cell line. Notably, neither thioacetohydrazide containing compounds **13b** or **14c** showed any cytotoxic activities against any of the three tested cell lines.

### 3.3. Molecular modelling and in silico study

#### 3.3.1. Docking study

The docking of compounds (**4a,b, 7c, 13b, and 14c**) into both the COX-1 (PDB code: 1EQG) and COX-2 (PDB code: 1CX2) binding sites were examined using Molecular Operating Environment (MOE) 2018 software<sup>58</sup>. For each compound, the pose with the best score was selected. The process was validated by re-docking SC-558 into the COX-2 active site and ibuprofen into the COX-1 active site, and their original conformations were reproduced (Score -9.39 and -7.56, RMSD: 1.34 Å<sup>0</sup> and 1.16 Å<sup>0</sup>, respectively).

The original main interactions of the co-crystallized ligand SC-558 into the COX-2 active site are four hydrogen bonds with Tyr355, His90, Arg513, and Arg120 and one hydrophobic interaction with Ser353. While within COX-1 active site, ibuprofen forms three hydrogen bonds with Arg120 and Tyr355. The COX-2 active site is larger than that of COX-1 owing to the presence of an extra side pocket. This extra pocket is bordered by Tyr355, His90, Gln192, and Arg513 (the last residue is altered in COX-1 by His513). The high selective COX-2 inhibitors usually bind to Arg513 through the sulphone of their sulphonamide groups<sup>13,59</sup>. The docking results for the selected compounds showed better scoring within COX-2 active site (-8.54 to -6.26) than that within the COX-1 active site (-6.42 to -2.06).

Compound **14c** showed the best score on COX-2 (-8.54) and was able to make hydrogen bonds with Arg513; these interactions have been reported to be responsible for the high selective inhibition of COX-2<sup>19,60</sup> for residues Ser353 (one of the key residues in the binding mode of SC-558) and Gly354 (Figure 5). Compound **13b** showed the highest score difference between COX-2 and COX-1 (-8.41, -2.06 respectively). These results are in line with the *in vitro* enzyme-binding assay and the high SI = 373 for the formation of hydrogen bond with Arg120 (one of the key residues in the binding mode of SC-558) within the COX-2 active site (Figure 6). Data provided in Supplementary Data Table 1.

Within the COX-2 active site, compound **4a** formed a hydrogen bond with Ala527 while compound **7c** made two hydrogen bonds with Val523 and Arg120 (one of the key residues in the binding mode of SC-558). Compound **4b** succeeded in making hydrophobic interactions with Ser353 (one of the key residues in the binding mode of SC-558) (Figures 7–9).

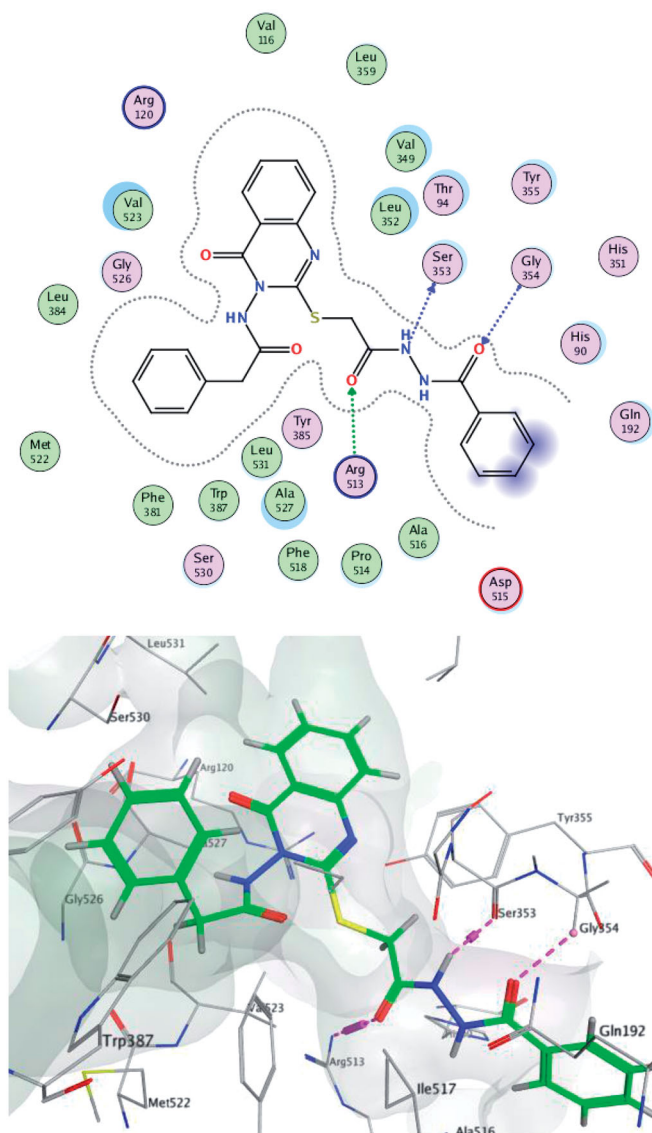


**Figure 5.** Two-/Three-dimensional (2-D, 3-D) binding interaction pattern of **14c** in the binding site of 1CX2.

Regarding COX-1 docking results and scores, compound **7c** failed to make any interaction with the surrounding residues. Compounds **4a, 4b, 13b, and 14c** made only one or two binding interactions with the surrounding residues including some with Arg120 (one of the key residues in the binding mode of ibuprofen) but with inferior scoring. This may be due to the bulkiness of the compounds which made them less preferred to fit into the COX-1 active site. Data provided in Supplementary Data Table 1.

The scoring for the poses of each compound with the COX-1/2 matches with our *in vitro* COX-1/COX-2 inhibition assay results and emphasise the occurrence of preferred binding between our compounds and COX-2 inhibition. Data provided in Supplementary Data Table 1.

#### 3.3.2. In silico prediction of pharmacokinetic and physiochemical properties

MOLINSPIRATION software<sup>46</sup> was used to predict the oral bioavailability of the selected new compounds (**4a,b, 7c, 13b, and 14c**) through Lipinski's rule of five and to determine the violation of

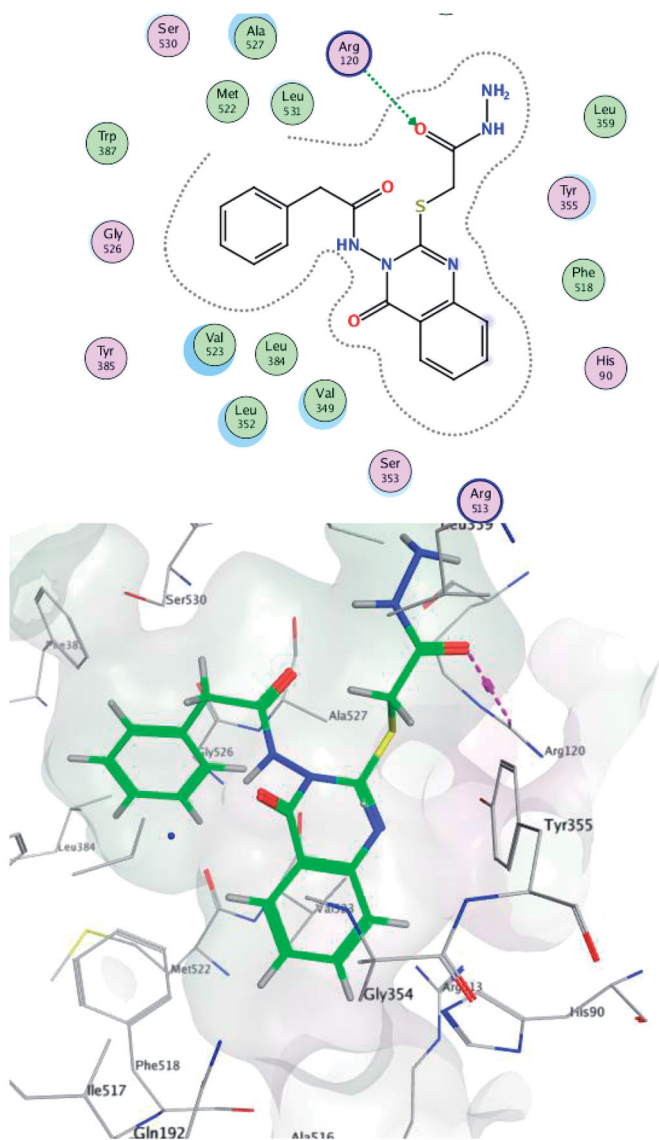


**Figure 6.** Two-/Three-dimensional (2-D, 3-D) binding interaction pattern of **13b** in the binding site of 1CX2.

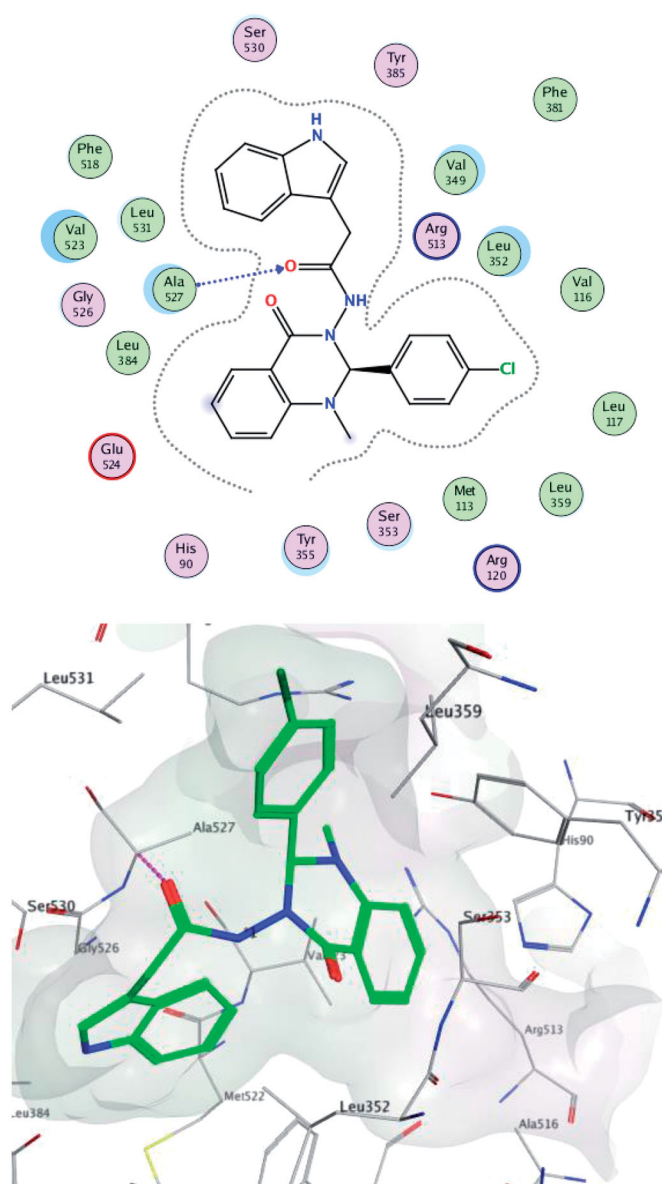


**Figure 7.** Two/Three-dimensional (2-D, 3-D) binding interaction pattern of **4a** in the binding site of 1CX2.

the rule. The topological polar surface area (TPSA)( $\text{\AA}^2$ ) is another parameter that provides information about bioavailability. Compounds with TPSA values below 140–150  $\text{\AA}^2$  are expected to have good bioavailability; while compounds with TPSA values lower than 70–80  $\text{\AA}^2$  are expected to cross the blood–brain barrier (BBB) and effectively target the CNS. The TPSA was also used in the calculation of oral bioavailability (%ABS) by the following previously reported equation: (%ABS) = 109–0.345 TPSA<sup>13,49</sup>. The TPSA and number of rotatable bonds (NROTB) both affect oral bioavailability in our animal studies. Compounds are expected to have high oral bioavailability if the NROTB and TPSA values are  $\leq 10$  and 140  $\text{\AA}^2$ , respectively. All data for selected new compounds provided in [Supplementary Data Table 2](#).

The selected compounds (**4a**, **b**, **13b**, and **14c**) did not violate Lipinski's rule, and therefore reveal suitable oral bioavailability. Only compound **7c** violated the parameters with  $\log P = 5.80$ . Compounds (**4b**, **7c**, **13b**, and **14c**) had TPSA values (range from 98.47–122.19) of less than 140  $\text{\AA}^2$  and more than 80  $\text{\AA}^2$ . These values indicate a diminished ability of these compounds to cross the BBB and therefore support the notion of limited potential CNS

adverse effects. The compound **4a** had TPSA value of 68.44 and was an exception to this.

The Pre-ADMET calculator<sup>47</sup> is used mainly for the prediction of permeability and absorption of synthesised drugs by two main models: the *in vitro* passive absorption through 2 parameter human epithelial colorectal adenocarcinoma cells (Caco2), and Mandin Dar by Canine Kidney (MDCK). Those two cell lines predict cell permeability as well as four other *in vivo* parameters: human intestinal absorption (HIA), blood brain barrier (BBB), plasma protein binding (PPB), and inhibition of cytochrome P450 2D6 (CYP2D6). ([Supplementary Data Table 3](#)).

All selected compounds (**4a**, **b**, **7c**, **13b**, and **14c**) have increased cell permeability for Caco2 over MDCK when compared with the reference compounds celecoxib, ibuprofen and indomethacin. For Caco2, the best compound was **4a** (34.04 nm/s) followed by **7c** (21.15 nm/s) and **4b** (19.75 nm/s); they showed relatively lower permeability when tested for MDCK (0.06–0.42 nm/s). For HIA, all the selected compounds showed similar readings that ranged from 91.51% to 96.97% and were

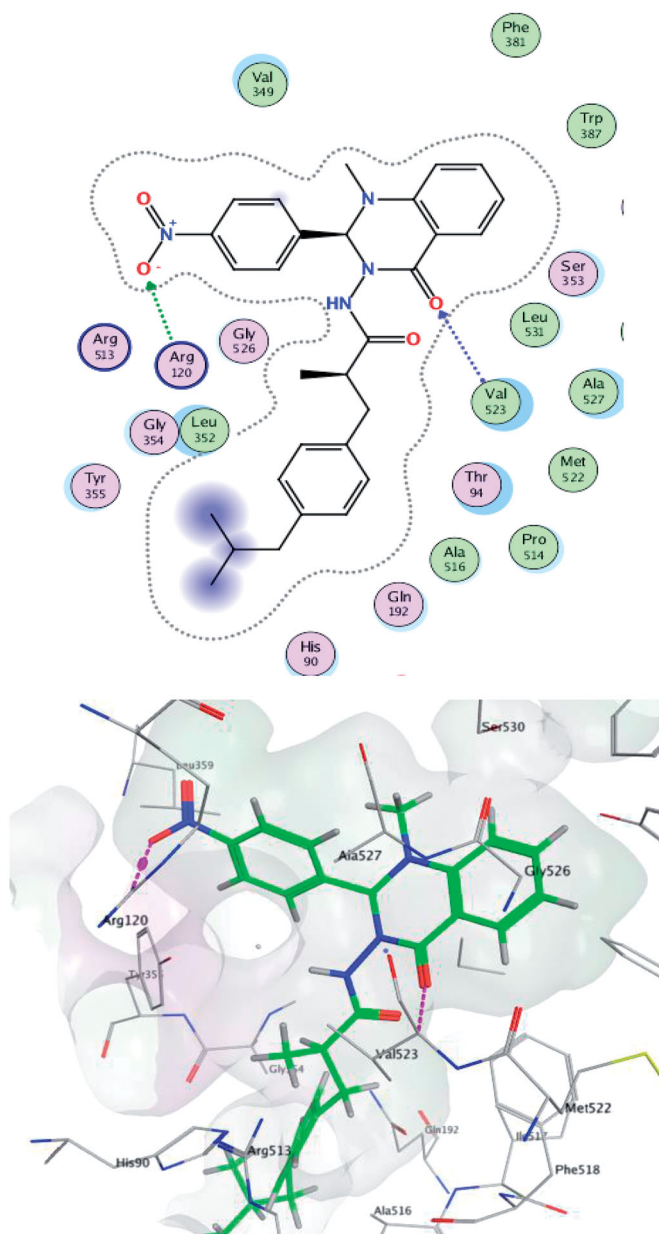


**Figure 8.** Two-/Three-dimensional (2-D, 3-D) binding interaction pattern of **7c** in the binding site of 1CX2.

comparable to the references, again supporting suitable oral bioavailability.

Our tested compounds showed low potential to cross the BBB, with BBB permeability values (0.03–0.08) which are similar to that of celecoxib (0.03). The exception to this low potential was found for compounds **4a** and **4b** which showed greater effectiveness for CNS penetration, having scored multiple-fold higher BBB permeability values of 4.07 and 0.31, respectively (Supplementary Data Table 3). Despite the low BBB penetration of celecoxib, it can reach concentrations in the CNS sufficient to effectively inhibit the COX-2 enzyme in that tissue. It is hypothesised that this mechanism is involved in celecoxib's central pain control and may explain its therapeutic efficacy in ischaemic brain injury, malignant brain tumours and neurodegenerative diseases such as Parkinson disease, amyotrophic lateral sclerosis, and Alzheimer disease. It is of interest, therefore, to identify analogues of celecoxib that have a similar efficacy profile but with improved BBB permeability<sup>61–63</sup>.

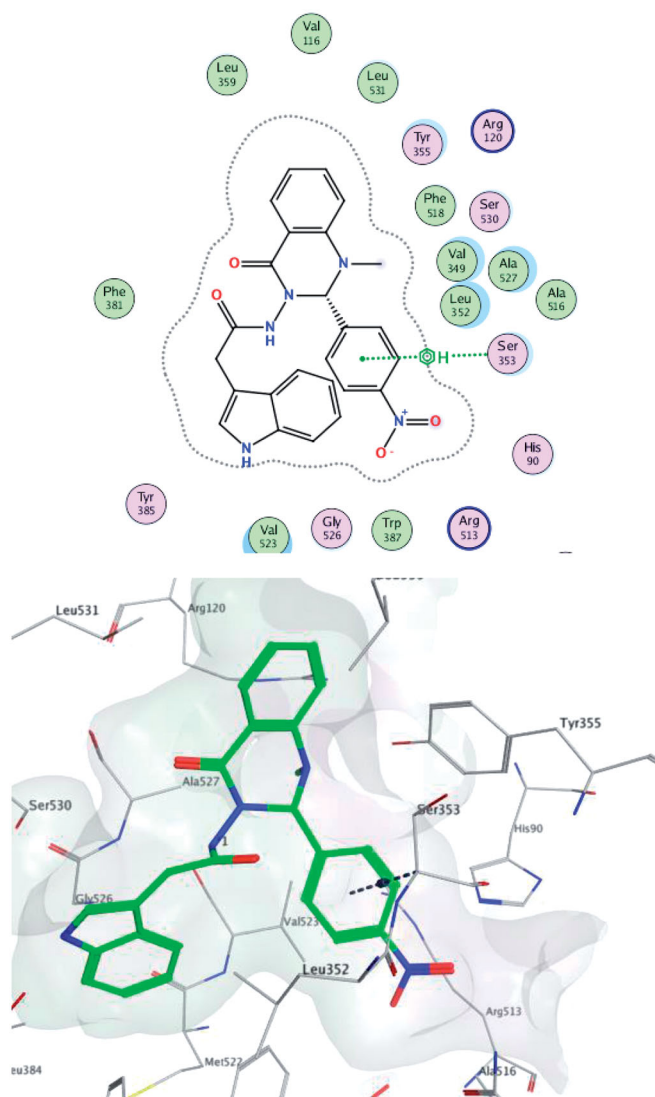


**Figure 9.** Two-/Three-dimensional (2-D, 3-D) binding interaction pattern of **4b** in the binding site of 1CX2.

Interestingly, the permeability scores of compounds **4a** and **4b** (4.07 and 0.31, respectively) predicted a greater BBB penetration compared to celecoxib (0.03). These compounds may resolve the CNS bioavailability limitations observed for celecoxib given these results. Further studies to explore the *in vivo* central anti-inflammatory potentials of both these compounds are currently in progress. This finding is especially relevant given that quinazolinone's ability to cross BBB as an anticonvulsant therapeutic is well reported<sup>64,65</sup>.

Notably, the selected compounds showed strong PPB-binding capacity that ranges from of 90.25% to 100%. Compound **14c** is the one with the highest score as it showed 100% PPB binding (Supplementary Data Table 3).

Lastly, similar to the three reference drugs (celecoxib, ibuprofen and indomethacin), the selected compounds (**4a**, **b**, **7c**, **13b**, and **14c**) do not inhibit the CYP2D6 enzyme; thus, they are expected to possess minimal drug-drug interactions either as inhibitors and/or inducers of this enzyme.

The results obtained by Osiris property explorer<sup>48</sup>, an online portal that predicts the possible toxicity of the tested compounds, showed that all our selected compounds exhibited drug-like behaviour with the exception of compound **13b**, which is



predicted to be associated with risk for tumorigenesis. Taken together, the results demonstrate that the newly synthesised compounds (**4a**, **b**, **7c**, **13b**, and **14c**) display acceptable physicochemical properties and fulfil Lipinski's rule of five. According to the pharmacokinetics predictions, these compounds are suitable future drug candidates.

#### 4. Conclusion

Novel quinazolinones conjugates with either indole acetamide (**4a-c**), ibuprofen (**7a-e**) or thioacetohydrazide (**13a,b** and **14a-d**) have been designed to be selective COX-2 inhibitors. All the designed compounds exhibited potent and selective COX-2 inhibitory profiles. The docking studies were in line with the *in vitro* COX1/2 assays. The compounds **4b**, **7c**, and **13b** showed nearly the same *in vivo* anti-inflammatory activity as ibuprofen and celecoxib and were more effective than indomethacin. Compounds **4a**, **b**, **7c**, and **14c** showed superior analgesic activity than that of celecoxib while **13b** showed the highest analgesic activity with complete abolishment of the pain response. Compounds **4a**, **b**, **7c**, **13b**, and **14c** exhibited greater inhibitory effects on LPS-induced NO and ROS production in RAW 264.7 macrophage cells than that of ibuprofen and indomethacin. Moreover, compared to celecoxib, compounds **13b** and **14a** showed greater inhibition of NO release and compound **7c** showed higher antioxidant potential (via inhibition of ROS production). The cell viability assay for anticancer activity revealed that compounds **4a**, **4b**, and **7c** had acceptable cytotoxic activity against HT29 cells, a cell line with moderate expression of COX-2 (IC<sub>50</sub> values = 13.42–66.67 μM). Collectively, our findings demonstrate that compounds **4a**, **b**, **7c**, **13b**, and **14c** represent potential candidates as selective COX-2 inhibitors with promising *in vivo* and *in vitro* anti-inflammatory and antioxidant activities. Additionally, compounds **4a** and **7c** showed an additional promising anticancer activity. Moreover, the *in silico* physicochemical and pharmacokinetic studies for these compounds showed promising results with excellent oral bioavailability, lower potential for drug-drug interactions, and overall acceptable physicochemical properties that fulfilled Lipinski's rule of five. Interestingly, compound **4a** and **4b** exhibited higher estimated BBB permeability compared with celecoxib. Due to this enhanced property, these compounds may be better able to overcome limitations to CNS bioavailability observed for celecoxib and to extend their clinical use as central inflammatory therapeutic targets. The findings of the current study suggest that compounds **4a**, **b**, **7c**, **13b**, and **14c** are all suitable potential drug candidates.

#### Acknowledgements

We are thankful to the efforts of Faculty of Pharmacy at Zagazig University for the purchase of MOE license version 2018 (Chemical Computing Group, Montreal, CA, USA). Our appreciation of the efforts of Dr. Waleed Ali, Biochemistry lab, Cairo General Hospital for his collaboration in *in vitro* COX-1/2 enzyme assays. Graphical abstract was created with BioRender.com.

#### Disclosure statement

The authors declare that they have no financial, conflict of interest, or personal relationships that may appear to hinder or affect this work. No potential conflict of interest was reported by the author(s).

#### Funding

This study was partially supported by the National Institute of General Medical Sciences of the National Institutes of Health under Award Number P20 GM121334 (D.G.R.). The content is solely the responsibility of the authors and does not necessarily represent the official views of the National Institutes of Health.

#### References

- Serhan CN. Treating inflammation and infection in the 21st century: new hints from decoding resolution mediators and mechanisms. *FASEB J* 2017;31:1273–88.
- Hassan GS, Rahman DEA, Abdelmajeed EA, et al. New pyrazole derivatives: synthesis, anti-inflammatory activity, cyclooxygenase inhibition assay and evaluation of mpges. *Eur J Med Chem* 2019;171:332–42.
- Motawi TK, Abd Elgawad HM, Shahin NN. Modulation of indomethacin-induced gastric injury by spermine and taurine in rats. *J Biochem Molecul Toxicol* 2007;21:280–8.
- Bindu S, Mazumder S, Bandyopadhyay U. Non-steroidal anti-inflammatory drugs (nsaids) and organ damage: a current perspective. *Biochem Pharmacol* 2020;180:(114)147.
- Rouzer CA, Marnett LJ. Cyclooxygenases: structural and functional insights. *J Lipid Res* 2009;50:S29–S34.
- Bozimowski G. A review of nonsteroidal anti-inflammatory drugs. *AANA J* 2015;83:425–33.
- Pereira-Leite C, Nunes C, Jamal SK, et al. Nonsteroidal anti-inflammatory therapy: a journey toward safety. *Med Res Rev* 2017;37:802–59
- Zhang Y, Wang Y, He C, et al. Pentafluorosulfonyl-substituted benzopyran analogues as new cyclooxygenase-2 inhibitors with excellent pharmacokinetics and efficacy in blocking inflammation. *J Med Chem* 2017;60:4135–46.
- Alaa A-M, Angeli A, El-Azab AS, et al. Synthesis and anti-inflammatory activity of sulfonamides and carboxylates incorporating trimellitimidates: dual cyclooxygenase/carbonic anhydrase inhibitory actions. *Bioorg Chem* 2019;84:260–8.
- El-Kerdawy MM, Ghaly MA, Darwish SA, et al. New benzimidazole derivatives as anti-inflammatory, antitumor active agents: synthesis, *in-vitro* and *in-vivo* screening and molecular modeling studies. *Bioorg Chem* 2019;83:250–61.
- Khatrri CK, Indalkar KS, Patil CR, et al. Novel 2-phenyl-4,5,6,7-tetrahydro[b]benzothiophene analogues as selective COX-2 inhibitors: design, synthesis, anti-inflammatory evaluation, and molecular docking studies. *Bioorg Med Chem Lett* 2017;27:1721–6.
- Abdelrahman MH, Youssif BG, Abdelazeem AH, et al. Synthesis, biological evaluation, docking study and ulcerogenicity profiling of some novel quinoline-2-carboxamides as dual coxs/lox inhibitors endowed with anti-inflammatory activity. *Eur J Med Chem* 2017;127:972–85.
- Sakr A, Kothayer H, Ibrahim SM, et al. 1,4-Dihydroquinazolin-3(2H)-yl benzamide derivatives as anti-inflammatory and analgesic agents with an improved gastric profile: design, synthesis, COX-1/2 inhibitory activity and molecular docking study. *Bioorg Chem* 2019;84:76–86.
- El-Sabbagh OI, Ibrahim SM, Baraka MM, Kothayer H. Synthesis of new 2,3-dihydroquinazolin-4(1H)-one derivatives for analgesic and anti-inflammatory evaluation. *Archiv Der Pharmazie* 2010;343:274–81.

15. Huang Y, Zhang B, Li J, et al. Design, synthesis, biological evaluation and docking study of novel indole-2-amide as anti-inflammatory agents with dual inhibition of cox and 5-lox. *Eur J Med Chem* 2019;180:41–50.
16. de Oliveira Moraes ADT, de Miranda MDS, Jacob ÍTT, et al. Synthesis, in vitro and in vivo biological evaluation, cox-1/2 inhibition and molecular docking study of indole-n-acylhydrazones derivatives. *Bioorg Med Chem* 2018;26:5388–96.
17. Abdellatif KR, Lamie PF, Omar HA. 3-methyl-2-phenyl-1-substituted-indole derivatives as indomethacin analogs: Design, synthesis and biological evaluation as potential anti-inflammatory and analgesic agents. *J Enzyme Inhibition Med Chem* 2016;31:318–24.
18. Kumar S, Kumar A, Agrawal A, Sahu JK. Synthesis, in vivo biological assessment and molecular docking study of some newer indole derivatives as cox 1/2 inhibitors. *J Mol Struct* 2021;1230:129831.
19. Kassab SE, Khedr MA, Ali HI, Abdalla MM. Discovery of new indomethacin-based analogs with potentially selective cyclooxygenase-2 inhibition and observed diminishing to pge2 activities. *Eur J Med Chem* 2017;141:306–21.
20. Alaa A-M, Abou-Zeid LA, ElTahir KEH, et al. Design, synthesis of 2,3-disubstituted 4(3H)-quinazolinone derivatives as anti-inflammatory and analgesic agents: COX-1/2 inhibitory activities and molecular docking studies. *Bioorg Med Chem* 2016; 24:3818–28.
21. Jan MS, Ahmad S, Hussain F, et al. Design, synthesis, in-vitro, in-vivo and in-silico studies of pyrrolidine-2,5-dione derivatives as multitarget anti-inflammatory agents. *Eur J Med Chem* 2020;186:111863.
22. Hardtmann GE, Koletar G, Pfister OR. The chemistry of 2h-3,1-benzoxazine-2,4(1h)dione (isatoic anhydrides) 1. The synthesis of n-substituted 2h-3,1-benzoxazine-2,4(1h)diones. *J Heterocyclic Chem* 1975;12:565–72.
23. Gadegoni H, Manda S. Synthesis and screening of some novel substituted indoles contained 1,3,4-oxadiazole and 1,2,4-triazole moiety. *Chinese Chem Lett* 2013;24:127–30.
24. Kumsi M, Poojary B, Lobo PL, et al. Synthesis, characterization and biological studies of some bioactive thiazolotriazole derivatives. *Zeitschrift Für Naturforschung B* 2010;65: 1509–15.
25. Hameed AH, Al-Majedy YK, Al-Amiery AA, Al-Sabti MD, Biochemical Division, Department of Applied Science, University of Technology, Baghdad-Iraq. Synthesis and characterization of some complexes of cr (iii), co (ii), ni (ii), and cu (ii) with (1-benzoyl-3-methyl-1hpyrazol-5 (4h)-one. *J Al-Nahrain Univ-Sci* 2009;12:31–7.
26. Mauri E, Rossi F, Sacchetti A. Simple and efficient strategy to synthesize peg-aldehyde derivatives for hydrazone orthogonal chemistry. *Polym Adv Technol* 2015;26:1456–60.
27. Ibrahim SM, Abo-Kul M, Soltan MK, Barakat W, Helal AS. Synthesis and Biological Screening of New Derivatives of 2, 3-dihydro quinazolin-4 (1H)-one and Benzotriazepin-5 (2H)-one for Central Nervous System Activity. *Med. Chem.* 2014;4:351-6.
28. Modi SKK, Vijay; Narang KS. Thiadiazoloquinazoline derivatives. ii. Synthesis of 2-aryl/alkyl-2,3-dihydro-5h,1,3,4-thiadiazolo[2,3b]quinazolin-5-ones. *Indian J Chem* 1970;8:710.
29. Nawrocka W, Wojcicka A, Nowicka A. Synthesis of novel 3-amino-2-(1h)-thioxo-4 (3h)-quinazolinone derivatives. Part 3. *Phosphorus Sulfur Silicon Relat Elements* 2012;187:79–87.
30. Phukan K, Ganguly M, Devi N. Mild and useful method for n-acylation of amines. *Synthetic Communications®* 2009;39: 2694–701.
31. Uddin MJ, Rao PP, Knaus EE. Design and synthesis of acyclic triaryl (z)-olefins: A novel class of cyclooxygenase-2 (cox-2) inhibitors. *Bioorg Med Chem* 2004;12:5929–40.
32. Alaa A-M, Abou-Zeid LA, ElTahir KEH, et al. Synthesis, anti-inflammatory, analgesic, cox-1/2 inhibitory activities and molecular docking studies of substituted 2-mercapto-4(3H)-quinazolinones. *Eur J Med Chem* 2016;121:410–21.
33. Council NR, Guide for the care and use of laboratory animals. 8th ed. Washington, DC: The National Academies Press 2010.
34. Sobeh M, Mahmoud MF, Petruk G, et al. Syzygium aqueum: a polyphenol- rich leaf extract exhibits antioxidant, hepatoprotective, pain-killing and anti-inflammatory activities in animal models. *Front Pharmacol* 2018;9:566.
35. Barberot C, Moniot A, Allart-Simon I, et al. Synthesis and biological evaluation of pyridazinone derivatives as potential anti-inflammatory agents. *Eur J Med Chem* 2018;146:139–46.
36. Cioli V, Putzolu S, Rossi V, et al. The role of direct tissue contact in the production of gastrointestinal ulcers by anti-inflammatory drugs in rats. *Toxicol Appl Pharmacol* 1979;50: 283–9.
37. Sobeh M, Mahmoud MF, Rezaq S, et al. Haematoxylin campechianum extract ameliorates neuropathic pain via inhibition of nf- $\kappa$ b/tnf- $\alpha$ /nox/inos signalling pathway in a rat model of chronic constriction injury. *Biomolecules* 2020;10: 386.
38. Sobeh M, Mahmoud MF, Rezaq S, et al. Salix tetrasperma roxb. Extract alleviates neuropathic pain in rats via modulation of the nf- $\kappa$ b/tnf- $\alpha$ /nox/inos pathway. *Antioxidants* 2019; 8:482.
39. Hegazi NM, Sobeh M, Rezaq S, et al. Characterization of phenolic compounds from eugenia supra-axillaris leaf extract using HPLC-PDA-MS/MS and its antioxidant, anti-inflammatory, antipyretic and pain killing activities *in vivo*. *Sci Rep* 2019;9:1–12.
40. Elhassanny AEM, Soliman E, Marie M, et al. Heme-dependent er stress apoptosis: a mechanism for the selective toxicity of the dihydroartemisinin, nsc735847, in colorectal cancer cells. *Front Oncol* 2020;10:965.
41. Soliman E, Van Dross R. Anandamide-induced endoplasmic reticulum stress and apoptosis are mediated by oxidative stress in non-melanoma skin cancer: receptor-independent endocannabinoid signaling. *Mol Carcinog* 2016;55:1807–21.
42. Talactac M, Lee JS, Moon H, et al. The antiviral effect of high-molecular weight poly-gamma-glutamate against Newcastle disease virus on murine macrophage cells. *Adv Virol* 2014;2014:301386.
43. Lee SY, Kim HJ, Han JS. Anti-inflammatory effect of oyster shell extract in lps-stimulated raw 264.7 cells. *Prev Nutr Food Sci* 2013;18:23–9.
44. Rezaq S, Abdel-Rahman AA. Central gpr109a activation mediates glutamate-dependent pressor response in conscious rats. *J Pharmacol Exp Ther* 2016;356:456–65.
45. Elhassanny AE, Soliman E, Marie M, et al. Van Dross R. Heme-dependent er stress apoptosis: A mechanism for the selective toxicity of the dihydroartemisinin, nsc735847, in colorectal cancer cells. *Frontiers in Oncology* 2020;10:965.
46. [www.molinspiration.com](http://www.molinspiration.com).
47. <https://preadmet.bmdrc.kr>.
48. <https://www.organic-chemistry.org/prog/peo/>.

49. Zhao YH, Abraham MH, Le J, et al. Rate-limited steps of human oral absorption and qsar studies. *Pharm Res* 2002;19: 1446–57.
50. Sharma V, Khan M. Prodrugs and mutual prodrugs: Synthesis of some new pyrazolone and oxadiazole analogues of a few non-steroidal anti-inflammatory drugs. *Die Pharmazie Int J Pharmaceu Sci* 2003;58:99–103.
51. Perkins DJ, Kniss DA. Blockade of nitric oxide formation down-regulates cyclooxygenase-2 and decreases pge2 biosynthesis in macrophages. *J Leukoc Biol* 1999;65:792–9.
52. Qi S, Feng Z, Li Q, et al. Myricitrin modulates nadph oxidase-dependent ros production to inhibit endotoxin-mediated inflammation by blocking the jak/stat1 and NOX2/p47phox pathways. *Oxid Med Cell Longev* 2017;2017: 9738745.
53. Zafarullah M, Li WQ, Sylvester J, Ahmad M. Molecular mechanisms of n-acetylcysteine actions. *Cell Mol Life Sci* 2003;60: 6–20.
54. Fujita M, Somasundaram V, Basudhar D, et al. Role of nitric oxide in pancreatic cancer cells exhibiting the invasive phenotype. *Redox Biol* 2019;22:101158.
55. Chan TA. Nonsteroidal anti-inflammatory drugs, apoptosis, and colon-cancer chemoprevention. *Lancet Oncol* 2002;3: 166–74.
56. Thun MJ, Henley SJ, Patrono C. Nonsteroidal anti-inflammatory drugs as anticancer agents: mechanistic, pharmacologic, and clinical issues. *J Natl Cancer Inst* 2002;94:252–66.
57. Valverde A, Peñarando J, Cañas A, et al. Simultaneous inhibition of egfr/vegfr and cyclooxygenase-2 targets stemness-related pathways in colorectal cancer cells. *PLOS One* 2015; 10:e0131363.
58. Molecular Operating Environment [MOE]; MOE, Version, 2018, Chemical Computing Group Inc., Montreal, Quebec, Canada <http://www.chemcomp.com>
59. Ghanim AM, Rezaq S, Ibrahim TS, et al. Novel 1,2,4-triazine-quinoline hybrids: the privileged scaffolds as potent multi-target inhibitors of LPS-induced inflammatory response via dual COX-2 and 15-LOX inhibition. *Eur J Med Chem* 2021; 219:113457.
60. Alaa A-M, El-Azab AS, Abou-Zeid LA, et al. Synthesis, anti-inflammatory, analgesic and cox-1/2 inhibition activities of anilides based on 5,5-diphenylimidazolidine-2,4-dione scaffold: molecular docking studies. *Eur J Med Chem* 2016;115: 121–31.
61. Dembo G, Park SB, Kharasch ED. Central nervous system concentrations of cyclooxygenase-2 inhibitors in humans. *Anesthesiology* 2005;102:409–15.
62. Novakova I, Subileau E-A, Toegel S, et al. Transport rankings of non-steroidal antiinflammatory drugs across blood-brain barrier *in vitro* models. *PLOS One* 2014;9:e86806.
63. Bauer B, Hartz AMS, Pekcec A, et al. Seizure-induced up-regulation of p-glycoprotein at the blood-brain barrier through glutamate and cyclooxygenase-2 signaling. *Molecul Pharmacol* 2008;73:1444–53.
64. Kothayer H, Ibrahim SM, Soltan MK, et al. Synthesis, *in vivo* and *in silico* evaluation of novel 2,3-dihydroquinazolin-4(1H)-one derivatives as potential anticonvulsant agents. *Drug Develop Res* 2019;80:343–52.
65. Noureldin NA, Kothayer H, Lashine ESM, et al. Synthesis, anticonvulsant activity, and SAR study of novel 4-quinazolinone derivatives. *Archiv Der Pharmazie* 2017;350:1600332.